The Fire Modeling Intercomparison Project (FireMIP) for CMIP7

Fang Li[1], David M. Lawrence[2], Brendan M. Rogers[3], Chantelle Burton[4], Huilin Huang[5], Yiquan Jiang[6], Johannes W. Kaiser[7], Matthew Kasoar[8], Hanna Lee[9], Ruby Leung[10], Lars Nieradzik[11], Aihui Wang[1], Daniel S. Ward[12], Ligeer Ce[1,13], Yangchun Li[1,13], Zhongda Lin[1], Apostolos Voulgarakis[14,7], and Yongkang Xue[15]

[1] State Key Laboratory of Earth System Numerical Modeling and Application, Institute of Atmospheric Physics, Chinese Academy of Sciences, Beijing, China
[2] NSF National Center for Atmospheric Research, Boulder, CO, USA
[3] Woodwell Climate Research Center, Falmouth, MA, USA
[4] Met Office Hadley Centre, Fitzroy Road, Exeter, UK
[5] University of Virginia, Charlottesville, VA, USA
[6] China Meteorological Administration–Nanjing University Joint Laboratory for Climate Prediction Studies, and Jiangsu Collaborative Innovation Center of Climate Change, School of Atmospheric Sciences, Nanjing University, Nanjing, China
[7] Atmosphere and Climate, The Climate and Environmental Research Institute NILU, Kjeller, Norway
[8] Leverhulme Centre for Wildfires, Environment and Society, Department of Physics, Imperial College London, London, UK
[9] Department of Biology, Norwegian University of Science and Technology, Trondheim, Norway
[10] Atmospheric, Climate, and Earth Sciences Division, Pacific Northwest National Laboratory, Richland, WA, USA
[11] Department of Physical Geography and Ecosystem Science, Lund University, Lund, Sweden
[12] Karen Clark & Company, Boston, MA, USA
[13] University of Chinese Academy of Sciences, Beijing, China
[14] School of Chemical and Environmental Engineering, Technical University of Crete, Chania, Greece
[15] Department of Geography, University of California Los Angeles, Los Angeles, CA, USA

Correspondence to: Fang Li (lifang@mail.iap.ac.cn)

Abstract. Fire is a global phenomenon and a key Earth system process. Extreme fire events have increased in recent years, and fire frequency and intensity are projected to rise across most regions and biomes, posing substantial challenges for ecosystems, the carbon cycle, and society. The Fire Model Intercomparison Project (FireMIP), launched in 2014, has contributed to advancing global fire modeling in Dynamic Global Vegetation Models (DGVMs) and improving understanding of fire's local drivers and local impacts on vegetation and land carbon budgets through land offline (i.e., uncoupled from the atmosphere) simulations. We now bring FireMIP into Coupled Model Intercomparison Project Phase 7 (CMIP7) to: (1) evaluate fire simulations in state-of-the-art fully coupled Earth system models (ESMs); (2) assess fire regime changes in the past, present, and future, and identify their primary natural and

anthropogenic forcings and causal pathways within the Earth system, including the associated uncertainties; and (3) quantify the impacts of fires and fire changes on climate, ecosystems, and society across Earth system components, regions, and timescales, and elucidate the underlying mechanisms. FireMIP in CMIP7 will advance the fire and fire-related modeling in fully coupled ESMs, and provide a quantitative, comprehensive, and process-based understanding of fire's role in the Earth system by using models that incorporate critical climate feedbacks and CMIP7 multi-model, multi-initial-condition, and multi-scenario ensemble. This protocol paper presents the motivation, scientific questions, experimental design and its rationale, model inputs and outputs, and the recommended analysis framework for FireMIP in CMIP7, providing guidance to Earth system modeling teams conducting simulations and informing communities studying fire, climate change, and climate solutions.

1. Introduction

Fire is a critical Earth system process, the primary form of terrestrial ecosystem disturbance on a global scale, and has been present since the emergence of terrestrial plants around 400 million years ago (Scott and Glasspool, 2006; Randerson et al., 2006; Bowman et al., 2009; Li et al., 2013). Each year, fire burns over 400 Mha of vegetated land (Giglio et al., 2018; Chuvieco et al., 2019; Chen et al., 2023), releasing 2–4 Pg of carbon globally along with large amounts of aerosols and trace gases (including greenhouse gases and air pollutants) and ozone/secondary-aerosol precursors (van der Werf et al., 2017; Wiedinmyer et al., 2023; Whaley et al., 2024; Kaiser et al., 2025). Fire is regulated by climate, vegetation, and human activities, and feeds back to them in multiple ways, both locally and remotely, across various temporal scales, forming intricate feedback loops (Bond-Lamberty et al., 2007; Jiang et al., 2016; Li and Lawrence, 2017; Li et al., 2017, 2019, 2022; Jones et al., 2022; Lou et al., 2023; Mao, 2024; Park et al., 2024; Harrison et al., 2025; Zhao et al., 2025).

Although global total burned area has declined over the past two decades (Andela et al., 2017), the frequency and intensity of extreme fire events (Cunningham et al., 2025), as well as forest fire emissions (Zheng et al., 2021), have increased. The reduction in global total burned area is largely due to decreased burning in tropical savannas and grasslands, which is mainly driven by human fire suppression (e.g., agricultural expansion increases landscape fragmentation and thus reduce fire spread, fire management) (Andela et al., 2017). By contrast, increases in extreme-fire occurrence and forest-fire emissions are

mainly linked to climate change and variability that enhance fuel drying and, in some regions, to fuel accumulation resulting from long-term fire suppression (Zheng et al., 2021; Cunningham et al., 2025). Importantly, burned area is projected to rise across most biomes, especially under the high-emission scenario and in extratropical regions (Li, 2021; Yu et al., 2022; UNEP, 2022; Sayedi et al., 2024; Bhattarai et al., 2025). This matters because fire can accelerate several Earth-system tipping elements, such as permafrost thaw, Amazon rainforest dieback, and boreal forest dieback, and affect Arctic sea-ice loss (Lenton et al., 2019). Fire can also limit effectiveness of climate solutions, including afforestation and reforestation, REDD+, and peatland rewetting.

Earth system models (ESMs) simulate the processes and feedbacks within and among the atmosphere, ocean, land, sea ice, and biosphere, and are essential for understanding historical changes in climate, environment, and ecosystems and for projecting the Earth's future (Scholze et al., 2013). ESMs have replaced climate models as the primary coupled models since the Coupled Model Intercomparison Project Phase 6 (CMIP6) (Dunne et al., 2025). Due to the critical role of fire in the Earth system, most ESMs now incorporate fire modeling. In CMIP6, 19 models submitted outputs of fire variables (Li et al., 2024a) versus 9 in CMIP5 (Kloster et al., 2017), and this number is expected to grow further in CMIP7. Furthermore, many ESMs have updated their fire schemes (e.g., Li et al., 2024b; Teixeira et al., 2025; Oberhagemann et al., 2025). Assessing the performance of CMIP7 ESMs in simulating fire and related variables is crucial for advancing fire-related process modeling.

Several studies have investigated fire changes across the past, present, and future and their local drivers. Over the past decades, global fire-regime changes are found to be driven mainly by human fire suppression (both direct and indirect, the latter through land-use-induced reduction in fuel continuity), enhanced by rising CO_2 levels that increase fuel load through CO_2 fertilization, and increasingly influenced by climate change (Andela et al., 2017; Li et al., 2018, 2019; Teckentrup et al., 2019; Burton et al., 2024; Scholten et al., 2024; Verjans et al., 2025). For the future, studies project an overall increase in global fires under CMIP5 and CMIP6 scenarios, particularly under the high emission scenario, mainly due to climate change including warming and increased lightning in Arctic-boreal regions and drying in the tropics (Kloster et al., 2017; Chen et al., 2021; Li, 2021; Wu et al., 2022; Byrne et al., 2024; Sayedi et al., 2024). Nevertheless, substantial uncertainties remain in the simulation of historical and future fire changes (Kloster et al., 2017; van Marle et al., 2017; Li et al., 2019; Li, 2021; Hamilton et al., 2024). In CMIP7, the Scenario Model Intercomparison Project (ScenarioMIP)

provides updated future scenarios that are more plausible than those in CMIP6 (van Vuuren et al., 2025). How fire regimes (i.e., the statistical characteristics of fire variables such as burned-area seasonality, spatial patterns, totals, and trends) will change under CMIP7 scenarios is unclear. In addition, many studies have used simulations from the Detection and Attribution Model Intercomparison Project (DAMIP) experiments in CMIP6 to attribute the impact of anthropogenic and natural forcings on climate (IPCC, 2021; Gillett et al., 2025), but far fewer have examined the downstream impacts on wildfires, and those that do are focused on the western United States (e.g., Zhuang et al., 2021). How anthropogenic and natural forcings have shaped historical global fire changes through climate and ecosystem processes remains unknown.

Fire impacts on the Earth system remain poorly quantified and understood. First, earlier studies primarily focused on specific components, such as biomass-burning effects on land carbon budgets or the radiative forcing and climate impacts of fire aerosols (Lasslop et al., 2019). Many other important fire impact processes, especially those across multiple Earth system components, are still unknown, for example, the global land-atmosphere-ocean carbon cycle, CH_4 emissions through affecting permafrost and wetland and their evolution in the atmosphere. Second, even for those processes that have been quantified, earlier estimates are likely inaccurate due to neglecting some critical climate feedbacks. Earlier studies quantified the fire impacts on land carbon and vegetation using land models driven by prescribed meteorological forcing, thereby neglecting fire-induced changes in surface climate (e.g., Li et al., 2014; Li and Lawrence, 2017; Ward et al., 2018; Arora and Melton, 2018; Lasslop et al., 2020; Pellegrini et al., 2023; Seo and Kim, 2023). Some coupled simulation studies adopted prescribed sea surface temperatures (SSTs) and/or sea ice coverage (e.g., Jiang et al., 2016; Grandey et al., 2016; Li et al., 2017a, b; Zou et al., 2020; Xu et al., 2021; Tian et al., 2022; Zhong et al., 2024; Blanchard-Wrigglesworth et al., 2025), which likely underestimated fire impacts due to the lack of air-sea interactions and sea-ice-albedo feedbacks (Jiang et al., 2020). Conversely, studies using a slab-ocean model, which lack horizontal heat transport, deep-water exchange, and ocean dynamics, may overestimate fire impacts (e.g., Jiang et al., 2020; Li et al., 2022; Zhao and Suzuki, 2019). Models without aerosol–cloud interactions (ACIs) have produced biased, sometimes even opposite-sign, fire-aerosol effects (e.g., Tosca et al., 2013; Yue and Unger, 2018; Li, 2020; Xu et al., 2021). Third, earlier coupled studies relied on a single model or a single initial-condition simulation, limiting characterization of model uncertainty and internal climate variability. For example, differences in the

strength of ACIs or aerosol–radiation interactions can produce large inter-model spread in estimated net fire-aerosol effects, ranging from net cooling to net warming (Landry et al., 2017; Jiang et al., 2020; Zhong et al., 2024; Blanchard- Wrigglesworth et al., 2025). Moreover, small perturbations to initial conditions can influence simulated climate states for decades to even over a century (Kay et al., 2015). Multi-model, multi-initial-condition, fully coupled simulations with critical climate feedbacks from CMIP7 therefore offer a unique opportunity to more robustly quantify fire's local and remote impacts across Earth system components and timescales, reveal the underlying mechanisms, and characterize the associated uncertainties.

The Fire Model Intercomparison Project (FireMIP), an international initiative launched in 2014, has worked to improve global fire modeling in DGVMs, understand local drivers of fires, and assess the influence of fires on vegetation, land carbon budgets, and, since 2020, on land and socioeconomic sectors as part of the Inter-Sectoral Impact Model Intercomparison Project (ISIMIP) (Hantson et al., 2016; Rabin et al., 2017; Frieler et al., 2024). Now integrated into CMIP7, FireMIP advances the study of fire's role in the Earth system using coupled model simulations. It contributes to improving fire and fire-related simulations in ESMs and addresses critical challenges in understanding fire dynamics, drivers, and impacts. CMIP7 FireMIP is also expected to provide useful insights for fire management, carbon accounting, air quality management, public health, land-use planning, and biodiversity protection. These insights link Earth system science to evidence-based policy making for risk management, ecosystem conservation, and sustainable development.

With the motivation and context outlined above, we describe in the following sections the scientific questions (Section 2), experimental design and rationale (Section 3), input and output variables (Section 4), and recommended analyses (Section 5), and conclude with the expected contributions to CMIP7 (Section 6).

2. Scientific questions

FireMIP in CMIP7 aims to address three fundamental fire-related scientific questions (Fig. 1):

(1) How well do state-of-the-art ESMs simulate global and regional fires?

Li et al. (2024) evaluated fire simulations from CMIP6 ESMs and found that they had addressed three critical issues identified in CMIP5: (i) simulated global burned area being less than half of observations,

(ii) failure to reproduce the high burned area fraction observed in Africa, and (iii) very weak fire seasonal variability. However, CMIP6 ESMs still underestimate the recent decline trend in global burned area, fail to capture the spring fire peak in the Northern mid-latitudes, and perform poorly in the Arctic-boreal zone. Since CMIP6, modeling groups have updated their ESMs (with fire-scheme improvements in some models), and more models will provide fire outputs in CMIP7. The first scientific question is therefore designed to assess how well state-of-the-art ESMs simulate fires, whether CMIP6 issues have been resolved, and what issues remain or newly emerge in CMIP7. It further aims to identify biases in fire and fire-related variables to guide future improvements in modeling fire–carbon–climate feedbacks, and to support model selection and bias correction for more reliable assessments of fire changes, drivers, and impacts addressed in Questions 2 and 3.

(2) How do fire regimes change in the past, present, and future (including uncertainties), and what are the dominant drivers?

This question focuses on two linked aspects: (i) characterizing fire changes in the past, present, and future, and (ii) attributing these changes. Regarding fire changes, CMIP6-simulated fire changes still have large uncertainties, and CMIP7 offers an opportunity to revisit them with improved models and scenarios. The uncertainties in fire change simulations can be quantified and separated into contributions from model uncertainty, internal climate variability (initial-condition uncertainty), and scenario uncertainty. Regarding attribution, earlier studies focused either on local, direct fire drivers (e.g., local weather and climate) or on attributing climate changes to anthropogenic versus natural forcings. CMIP7 FireMIP integrates the two by analyzing how anthropogenic and natural forcings

shape global fire changes by altering local, direct fire drivers.

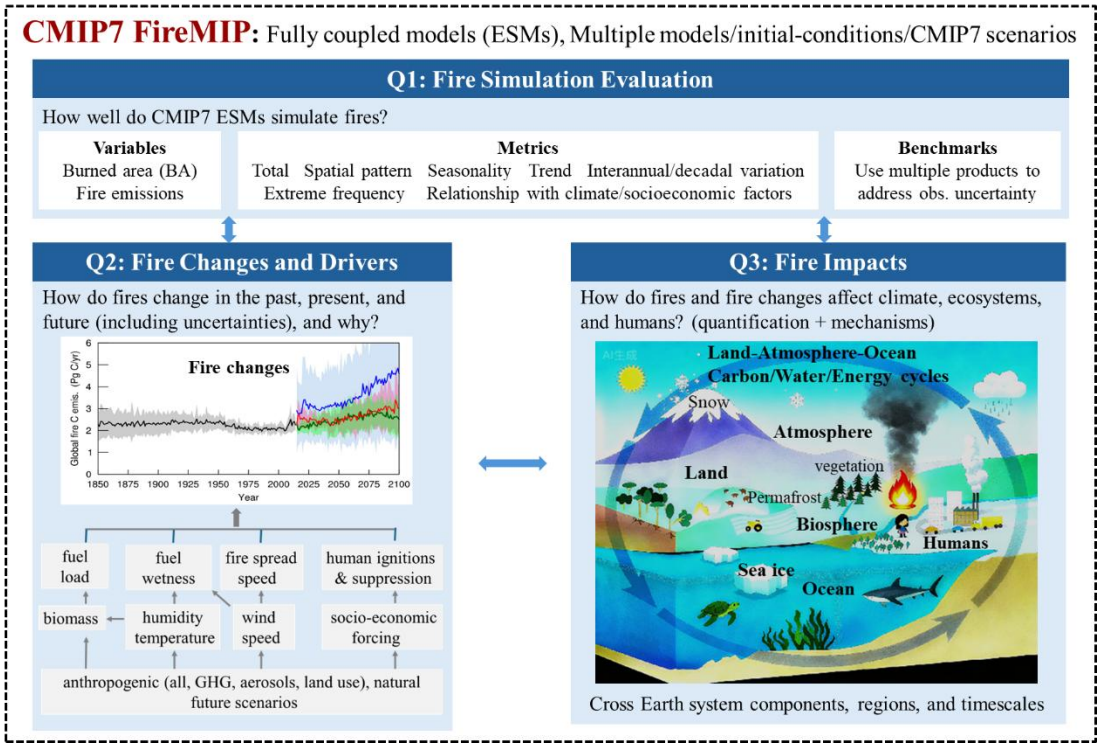

Figure 1. Scientific questions and proposed analyses for FireMIP in CMIP7. The fire-change panel is adapted from Li (2021).

(3) How do fires and fire changes impact climate, ecosystems, and humans?

This question explores the impacts of fires and changes in fire regimes on the land-atmosphere-ocean carbon, water, and energy cycles; vegetation distribution and structure; atmospheric composition, chemistry, and circulation; surface climate (e.g., temperature, precipitation, humidity, wind speed); the cryosphere (permafrost extent and active-layer depth, sea ice extent and thickness, snow cover and depth); air quality; and human activities. It also investigates the associated uncertainties, and the feedback mechanisms that cascade across Earth-system components. For example, it examines how fires influence climate and the carbon cycle through changes in land ecosystems and emissions of aerosols and trace gases, and how these changes, in turn, affect the spatial and temporal variability of fires. Addressing this question can also help clarify the potential role of fires in triggering or amplifying tipping-point transitions in boreal forests, the Amazon rainforest, permafrost, and Arctic sea ice.

3. Experimental design

CMIP7 FireMIP comprises three experiment groups (Table 1) designed to address the scientific questions outlined above. The design follows the principle of minimizing computational burden while effectively addressing the scientific questions, aiming to encourage broad participation from the modeling community, given that fully coupled ESM runs are very expensive. The tier-1 (required) experiments in Groups 1 and 2 come from CMIP7 Diagnostic, Evaluation and Characterization of Klima (DECK) and Assessment Fast Track (AFT) experiments. To participate in FireMIP, modeling groups must output two fire variables (i.e., burned area fraction and fire carbon emissions) from these simulations. Group 3 (Fire impacts) experiments are specific to FireMIP. Modeling groups are required to provide the hist-no-fire simulation and are encouraged to conduct one to three additional Group 3 experiments based on scientific interest and available resources. For coupled simulations, running at least three initial-condition ensemble members for each experiment is strongly recommended to improve the robustness of the assessment, given the role of internal climate variability, and is consistent with DECK and AFT requirements.

Group 1 experiments are used to evaluate fire simulations and identify biases (Table 2). The experiments include concentration-driven (historical) or emission-driven (esm-historical) coupled model simulations, and historical land model offline simulations (land-hist). Fire simulations in coupled models will be assessed to identify improvements compared to CMIP6 and to highlight issues that will guide further model development. Besides, the possible sources of improvement and bias (from land modeling, atmosphere modeling, or air-land coupling) can be identified by comparing coupled (historical or esm-historical) with land only (land-hist) simulations.

Group 2 experiments are used to assess fire changes and drivers. These experiments include: (2.1) simulations for 2022–2100 under high (h, policy failure), medium (m, current policy), medium-low (ml, delayed mitigation policy), and low (l, aligned with Paris agreement) emission scenarios; and (2.2) a historical sensitivity simulation (hist-nat) similar to historical and esm-historical, driven by time-varying solar and volcanic forcings, with all other forcings fixed at their 1850 levels. In addition, lower-priority simulations in FireMIP include (2.3) 1850–2022 simulations as historical and esm-historical with only anthropogenic aerosols (hist-aer), greenhouse gases (hist-GHG), and land use (hist-lu) varying in time, with other forcings fixed at 1850 levels, and (2.4) 2022–2100 simulations under very low emissions after limited overshoot (vllo) and high overshoot (vlho). Here, “overshoot” denotes the magnitude by which global warming temporarily exceeds the 1.5°C target level during the 21st century (Van Vuuren et al.,

2025).

Table 1. Description of CMIP7 FireMIP experiments.

Group	Experiment ID	Description	Priority
1. Fire Simulation Evaluation	(1.1) historical/esm-historical (DECK)	1850–2021 historical concentration- or emission (esm)-driven coupled simulations	1
	(1.2) land-hist (AFT; LMIP tier-1)	1850–2021 historical offline land-model simulations	3
2. Fire Changes and Drivers	(2.1) scen7-hc/esm-scen7-h scen7-mc/esm-scen7-m scen7-mlc/esm-scen7-ml scen7-lc/esm-scen7-l (AFT; ScenarioMIP tier-1)	2022–2100 concentration-driven or emission- driven coupled simulations under high (h, policy failure), medium (m, current policy), medium-low (ml, delayed mitigation policy), and low (l, Paris Agreement) emission scenarios	1
	(2.2) hist-nat (AFT; DAMIP tier-1)	same as historical/esm-historical, but with time-varying solar and volcanic forcings, while other forcings fixed at 1850 levels	1
	(2.3) hist-aer & hist-GHG (AFT; DAMIP tier-1) hist-lu (DAMIP tier-1)	same as historical/esm-historical, but with time-varying anthropogenic aerosols (hist-aer), greenhouse gases (hist-GHG), and land use (hist-lu), while other forcings fixed at 1850 levels	2
	(2.4) scen7-vlloc/ esm-scen7-vllo scen7-vlhoc/ esm-scen7-vlho (AFT; ScenarioMIP tier-1)	2022–2100 coupled simulations under very low emissions after limited overshoot (vllo) and high overshoot (vlho) scenarios	3
3 Fire Impacts	(3.1) hist-no-fire	1850–2021 historical coupled simulations with fires set to zero	1
	(3.2) hist-no-fireaero	branching from historical/esm-historical no later than 1920, with fire aerosols set to zero thereafter	2
	(3.3) scen7-h-no-firechange	2022–2060 simulations as scen7-h, but with fires fixed at the 2001–2020 average	2
	(3.4) scen7-h-no-fireaerochange	2022–2060 simulations as scen7-h, but with fire aerosol emission fixed at the 2001–2020 average	2

Priority: 1 (required); 2 (recommended); 3 (optional)

Table 2. Scientific objectives of experiments and inter-experiment comparisons.

Experiments and comparisons	Scientific objectives
1. Fire Simulation Evaluation	
historical/esm-historical	evaluate fire-simulation and assess historical fire changes
historical/esm-historical vs. land-hist	diagnose sources of bias and improvements
2. Fire Changes and Drivers	
historical/esm-historical	assess historical fire changes
historical/esm-historical vs.	assess future fire changes and factors across scenarios:
scen7-hc/esm-scen7-h	high (h)
scen7-mc/esm-scen7-m	medium (m)
scen7-mlc/esm-scen7-ml	medium-low (ml)
scen7-lc/esm-scen7-l	low (l)
scen7-vlloc/esm-scen7-vllo	very low emissions after limited overshoot (vllo)
scen7-vlhoc/esm-scen7-vlho	very low after high overshoot (vlho)
historical/esm-historical vs.	attribute historical fire changes to changes in
hist-nat	natural and anthropogenic forcings
hist-aer	anthropogenic aerosol emissions (aer)
hist-GHG	anthropogenic greenhouse gas emissions (GHG)
hist-lu	or anthropogenic land use (lu)
3. Fire Impacts	
historical/esm-historical vs.	
hist-no-fire	assess impacts of fires
hist-no-fireaero	or fire aerosols during the historical period
scen7-hc/esm-scen7-h vs.	
scen7-h-no-firechange	assess impacts of fire changes
scen7-h-no-fireaerochange	or fire aerosol changes under high emission scenario

Experiments (2.1) and (2.3), together with the historical and esm-historical simulations in Group 1, are used to assess how fire and fire emissions have changed during the historical period and how they will evolve under current-policy and failed-policy futures, as well as under varying levels of mitigation-policy success (Table 2). Comparing experiments (2.2) and (2.4) with the historical and esm-historical simulations enables the assessment of how natural and anthropogenic forcings influence fires and isolates the effects of anthropogenic forcings, including aerosols, greenhouse gases, and land use (Table 2).

Group 3 experiments are designed to quantify the impacts of fires, fire aerosols, future fire changes, and future changes in fire aerosols, respectively, and to explore the underlying mechanisms. Among them, (3.1) hist-no-fire is an idealized “no-fire world” historical (1850–2021) simulation used to quantify fire

impacts. In models with prescribed fire emissions, burned area in the code and prescribed fire-emission fluxes in the forcing dataset are set to zero; in models with interactive fire modules, burned area is set to zero and fire emissions are consequently diagnosed as zero. CanESM simulations indicate that the global vegetation carbon pool and land surface air temperature require approximately 150–200 years and nearly 50 years, respectively, to reach their new no-fire equilibria after fires are switched off (V. K. Arora, 2025, personal communication). Therefore, we require an 1850 no-fire spin-up as the initial state to prevent artificial trends arising from climate and carbon adjustments before equilibrium. We request that modeling groups document whether they use prescribed or interactive fire emissions to enable stratified analyses by configuration in the impact assessment.

Experiment (3.2) hist-no-fireaero branches from the historical or esm-historical simulation no later than 1920, with fire-aerosol emissions set to zero thereafter. The year 1920 is chosen to provide at least 70 years of no-fire-aerosol spin-up, allowing the isolation of present-day fire-aerosol impacts. The spin-up length is informed by evidence that the global water cycle in CESM2 reaches no-fire-aerosol equilibrium after about 70 years (Li et al., 2022), and that the global vegetation and soil carbon pools require roughly 50 and 80 years, respectively, to equilibrate or show only minor slow changes in the CMIP6 global deforestation experiment (Boysen et al., 2020). Comparing the present-day averages, seasonality, recent trends, and decadal/interannual variations of target variables from experiments (3.1) and (3.2) with the historical or esm-historical simulations enables the assessment of fire impacts and fire-aerosol impacts, respectively (Table 2).

Additionally, Experiments (3.3) scen7-h-nofirechange is a 2022–2060 simulation, the same as scen7-h, but with burned area and fire emissions fixed at their 2001–2020 average. It requires burned area to be prescribed as an input field using each model's own 2001–2020 average derived from its historical simulations, and in models without interactive fire-emission modules, fire emissions in the 2022–2060 input files must likewise be replaced with the 2001–2020 average. Experiment (3.4) scen7-h-no-fireaerochange is a 2022–2060 simulation, the same as scen7-h, but with fire aerosol emissions in the inputs fixed at the 2001–2020 average, which is not applicable to ESMs with interactive fire-emission modules. Comparing Experiments (3.3) and (3.4) with the scen7-h simulations for 2022–2060 facilitates assessing the impacts of future changes in fires and fire aerosols, respectively, under a high-emission scenario (Table 2).

The experimental priority tiers in CMIP7 FireMIP follow the CMIP7/CMIP data-request convention.

Priority 1 (required) is the minimum set needed to meet the FireMIP objectives (fire evaluation; fire changes and drivers; fire impacts) and to maximize broad community utility. Priority 2 (recommended) includes important experiments that provide a more complete and robust assessment (e.g., improved attribution by separating anthropogenic forcings; impact analyses of fire aerosols, fire changes, and fire aerosol changes), but may not be feasible for all modeling centers due to computational cost or other constraints. Priority 3 (optional) includes additional experiments that further support the FireMIP objectives and are of interest to the community, which are undertaken as resources allow.

Experiments (2.3) (hist-aer, hist-GHG, hist-lu) can provide a more detailed attribution of historical fire changes to specific anthropogenic drivers (aerosols, greenhouse gases, and land use), thereby strengthening the assessment of Scientific Question 2 (Fire changes and drivers). However, the core separation of natural versus anthropogenic influences can be addressed using (2.1) hist-nat relative to the historical experiment, so (2.3) is lower priority. Similarly, experiments (2.4) (scen7-vlloc/esm-scen7-vllo and scen7-vlhoc/esm-scen7-vlho) are designed to add overshoot-specific insight, but the core assessment of future fire changes across alternative scenarios and associated drivers can be addressed with (2.2) (scen7-h/m/ml/l), and (2.4) is therefore also assigned a lower priority.

4. Inputs and outputs

4.1 Inputs

Fire-specific inputs that ESM may use include: (1) population density, for modeling ignitions and human direct fire suppression; (2) lightning frequency for natural ignitions; (3) GDP for human direct fire suppression; (4) peatland area fraction, for peat fire modeling; (5) peak month of agricultural fires for timing of agricultural waste burning; and (6) fire-sourced trace gas and aerosol emissions representing part of fire impacts (Table 3).

Whether a given variable is needed depends on the model's fire parameterization scheme (Table 3). For example, ESMs without modeling direct human effects on fires needn't population density, GDP, or peak month of agricultural fires. Similarly, models that do not simulate peat fires do not require peatland area fraction. For ESMs that activate the interactive fire-emission module (i.e., simulate fire emissions and pass to the atmospheric model) and model lightning, prescribed fire emissions and lightning frequency are not needed.

Table 3. Overview of potential fire-specific inputs used in ESMs.

Variables	Role	Module/Process	Required when…
Population density	Calculate anthropogenic ignitions and human direct fire suppression	Fire occurrence Fire spread	Human direct fire effects are modeled
Lightning frequency	Calculate natural ignitions	Fire occurrence	Natural ignitions are modeled and lightning frequency are prescribed
GDP	Calculate human direct fire suppression/ management	Fire occurrence Fire spread	Economic impact on fire suppression considered
Peatland area fraction	Define peat-fire-prone area	Peat fires	Peat fires are modeled
Peak month of agricultural fires	Define timing or agricultural waste burning	Agricultural fires	Agricultural fires are modeled and not set to zero or as grass fires
Fire-sourced trace gas and aerosol emissions	Calculate impacts of fire emissions on atmosphere	Fire emissions-atmosphere	Fire emissions are prescribed

Historical gridded population density data (1850–2025; Paprotny and Hawker, 2025) and fire emission data (1750–2023; van Marle and van der Werf, 2025) are provided by CMIP7 forcing group and available through https://input4mips-cvs--350.org.readthedocs.build/en/350/database-views/input4MIPs_delivery-summary.html. Future population density and fire aerosol emission datasets are under development. Because CMIP7 will not provide forcing data for inputs (2–5), models may use their default forcing datasets. Standardized, consistent datasets (e.g., the CESM3 input set; will be available via https://wcrp-cmip.org/mips/firemip/) is recommended to reduce uncertainty..

4.2 Output variables

The variables requested by CMIP7 FireMIP are classified into two categories: (1) fire variables and (2) variables of fire drivers and impacts. The fire variables, specifically burned area fraction and fire carbon emissions, are the highest priority (Table 4). Here, fire carbon emissions" refers to the total carbon emitted by fires across carbon-containing species (CO2, CO, CH4, NMVOCs, carbonaceous aerosols), rather than CO2 alone. Burned area fraction and fire carbon emissions are essential for evaluating fire simulations and assessing fire-regime changes. They are default fire outputs that are most consistently available across ESMs. Outputs of additional fire-related variables (e.g., fire counts, fire intensity, fire size, fire speed, fire duration, land-cover-type–specific fire carbon emissions, and speciated trace-gas and

aerosol emissions) are encouraged where available.

Table 4. CMIP7 FireMIP outputs: fire variables

Name	Description	Branded name	Unit	#Dims	Frequency
burntFractionAll	Burned Area Fraction	burntFractionAll_tavg-u-hxy-u	% mon^{-1}	3	monthly
fFire	Fire Carbon Emissions	fFire_tavg-u-hxy-lnd	kg C m^{-2} s^{-1}	3	monthly

The fire driver and impact variables include land-atmosphere-ocean carbon cycle variables (Table 5) as well as other land (vegetation structure, vegetation distribution, land nitrogen fluxes and pools, land hydrothermal, snow characteristics), atmosphere (meteorology, atmospheric circulation, physics, composition, and chemistry), and ocean and sea-ice variables (Table 6). These variables will be used to evaluate model accuracy in capturing fire-ecosystems and fire-climate relationships, and to investigate the drivers of fire-regime changes and fire impacts.

These variables of fire drivers and impacts are selected because previous studies show that they (1) respond to natural and anthropogenic forcings, and can also influence fuel load, fuel flammability, and/or fire spread (IPCC, 2021; Gillett et al., 2025); (2) are significantly affected by fires at global or regional scales, e.g., land carbon budgets and vegetation (e.g., Bond-Lamberty et al., 2007; Li et al., 2014; Yue and Unger, 2018; Lasslop et al., 2020; Zou et.al., 2020; Seo and Kim, 2023), land nitrogen fluxes and pools (Beaudor et al., 2025), surface climate (e.g., Jiang et al., 2016; Li and Lawrence 2017; Li et al., 2017), land–atmosphere energy exchange (e.g., Li et al., 2017), water cycle (Li et al., 2022), CH_4 cycle (Tian et al., 2016), dust emissions (Yu and Ginoux, 2022), atmospheric composition and chemistry (e.g., Ward et al., 2012; Li et al., 2019; Jiang et al., 2020), large-scale atmospheric circulation (Li et al., 2022; Scholten et al., 2022), sea ice and snow (e.g., Li et al., 2022; Zhong et al., 2024), permafrost (Talucci et al., 2025), sea-surface temperature (Li et al., 2022), and marine ecosystems (Liu et al., 2022; Riera and Pausas, 2023); (3) are likely affected by the fire-induced changes listed in (2) (i.e., downstream variables), such as atmosphere and ocean carbon and energy; and (4) are needed to diagnose the response and influence mechanisms (i.e., intermediate variables), such as ocean currents.

Table 5. CMIP7 FireMIP outputs: land-atmosphere-ocean carbon cycle variables

Name	Description	Branded name	Unit	#Dims	Frequency
gpp	Gross Primary Productivity	gpp_tavg-u-hxy-lnd	kg C m^{-2} s^{-1}	3	monthly
ra	Autotrophic Respiration	ra_tavg-u-hxy-lnd	kg C m^{-2} s^{-1}	3	monthly
rh	Heterotrophic Respiration	rh_tavg-u-hxy-lnd	kg C m^{-2} s^{-1}	3	monthly
fLuc	Land-Use Change carbon emissions	fLuc_tavg-u-hxy-lnd	kg C m^{-2} s^{-1}	3	monthly
npp	Net Primary Productivity	npp_tavg-u-hxy-lnd	kg C m^{-2} s^{-1}	3	monthly
nep	Net Ecosystem Productivity	nep_tavg-u-hxy-lnd	kg C m^{-2} s^{-1}	3	monthly
nbp	Net Biospheric Productivity	nbp_tavg-u-hxy-lnd	kg C m^{-2} s^{-1}	3	monthly
cLeaf	Carbon mass in leaves	cLeaf_tavg-u-hxy-lnd	kg C m^{-2}	3	monthly
cStem	Carbon Mass in stems	cStem_tavg-u-hxy-lnd	kg C m^{-2}	3	monthly
cRoot	Carbon Mass in Roots	cRoot_tavg-u-hxy-lnd	kg C m^{-2}	3	monthly
cProduct	Carbon Mass in Products of Land-Use Change	cProduct_tavg-u-hxy-lnd	kg C m^{-2}	3	monthly
cVeg	Carbon Mass in Vegetation	cVeg_tavg-u-hxy-lnd	kg C m^{-2}	3	monthly
cLitter	Carbon Mass in Litter	cLitter_tavg-u-hxy-lnd	kg C m^{-2}	3	monthly
cSoil	Carbon Mass in Soil	cSoil_tavg-u-hxy-lnd	kg C m^{-2}	3	monthly
co2	Mole Fraction of CO2 in air	co2_tavg-p19-hxy-air	mol mol^{-1}	3	monthly
fgco2	Surface Downward Mass Flux of Carbon as CO2	fgco2_tavg-u-hxy-sea	kg C m^{-2} s^{-1}	3	monthly
spco2	Surface Aqueous Partial Pressure of CO2	spco2_tavg-u-hxy-sea	Pa	3	monthly
dissic	Dissolved Inorganic Carbon Concentration	dissic_tavg-ol-hxy-sea	mol m^{-3}	3	monthly
dissoc	Dissolved Organic Carbon Concentration	dissoc_tavg-ol-hxy-sea	mol m–3	3	monthly
intnpp	NPP by Phytoplankton	intpp_tavg-u-hxy-sea	Kg C m^{-2}	3	monthly

The variables in Tables 4–6 are included in the CMIP7 DECK and AFT variable requests. It is acceptable for some variables to be absent if the model does not include the corresponding component or process, such as the ocean ecosystem, terrestrial nitrogen cycle, CH_4 cycle, groundwater, or air-quality (e.g., surface $PM_{2.5}$ and O_3 concentrations).

Some variables in Table 6 are listed with daily or hourly frequencies because corresponding monthly variables are unavailable in the CMIP7 variable list. If modeling teams provide monthly outputs for these variables, that is acceptable. CMIP7 FireMIP does not have specific requirements for spatial resolution.

Table 6. CMIP7 FireMIP outputs: other land, atmosphere, ocean, and sea ice variables

Name	Description	Branded name	Unit	#Dims	frequency
Land					
lai	Leaf Area Index	lai_tavg-u-hxy-lnd	unitless	3	monthly
vegHeight	Height of Canopy	vegHeight_tavg-u-hxy-veg	m	3	monthly
treeFrac	Tree Cover Percentage	treeFrac_tavg-u-hxy-u	%	3	monthly
grassFrac	Grass Area Percentage	grassFrac_tavg-u-hxy-u	%	3	monthly
shrubFrac	Shrub Area Percentage	shrubFrac_tavg-u-hxy-u	%	3	monthly
cropFrac	Crop Area Percentage	cropFrac_tavg-u-hxy-u	%	3	monthly
baresoilFrac	Bare Soil Area Percentage	baresoilFrac_tavg-u-hxy-u	%	3	monthly
fNgasFire	Nitrogen Lost to the Atmosphere from Fire	fNgasFire_tavg-u-hxy-lnd	kg N m^{-2} s^{-1}	3	monthly
fNdep	Nitrogen deposition	fNdep_tavg-u-hxy-lnd	kg N m^{-2} s^{-1}	3	monthly
Fbnf	Biological Nitrogen Fixation	fBNF_tavg-u-hxy-lnd	kg N m^{-2} s^{-1}	3	monthly
fNleach	Nitrogen Loss to Leaching or Runoff	fNleach_tavg-u-hxy-lnd	kg N m^{-2} s^{-1}	3	monthly
fNup	Total Plant Nitrogen Uptake	fNup_tavg-u-hxy-lnd	kg N m^{-2} s^{-1}	3	monthly
nVeg	Vegetation Nitrogen Mass	nVeg_tavg-u-hxy-lnd	kg N m^{-2}	3	monthly
nLitter	Nitrogen Mass in Litter	nLitter_tavg-u-hxy-lnd	kg N m^{-2}	3	monthly
nSoil	Nitrogen Mass in Soil	nSoil_tavg-u-hxy-lnd	kg N m^{-2}	3	monthly
nMineral	Soil Mineral Nitrogen	nMineral_tavg-u-hxy-lnd	kg N m^{-2}	3	monthly
tsl	Soil temperature	tsl_tavg-sl-hxy-lnd	K	4	monthly
mrsol	Water Content of Soil Layer	mrsol_tavg-sl-hxy-lnd	kg m^{-2}	4	monthly
mrso	Total Soil Moisture Content	mrso_tavg-u-hxy-lnd	kg m^{-2}	3	monthly
evspsblveg	Canopy Evaporation	evspsblveg_tavg-u-hxy-lnd	kg m^{-2} s^{-1}	3	monthly
evspsblsoi	Soil Evaporation	evspsblsoi_tavg-u-hxy-lnd	kg m^{-2} s^{-1}	3	monthly
tran	Transpiration	tran_tavg-u-hxy-lnd	kg m^{-2} s^{-1}	3	monthly
evspsbl	Evapotranspiration	evspsbl_tavg-u-hxy-u	kg m^{-2} s^{-1}	3	monthly
mrro	Total Runoff	mrro_tavg-u-hxy-lnd	kg m^{-2} s^{-1}	3	monthly
mrros	Surface Runoff	mrros_tavg-u-hxy-lnd	kg m^{-2} s^{-1}	3	monthly
rivo	River Discharge	rivo_tavg-u-hxy-lnd	m^3 s^{-1}	3	daily
friver	Water Flux into Sea Water from Rivers	friver_tavg-u-hxy-sea	kg m^{-2} s^{-1}	3	monthly
dgw	Change in Groundwater	dgw_tavg-u-hxy-lnd	kg m^{-2}	3	daily
wtd	Water Table Depth	wtd_tavg-u-hxy-lnd	m	3	daily
prveg	Canopy Interception	prveg_tavg-u-hxy-lnd	kg m^{-2} s^{-1}	3	monthly
rlds	Surface Downwelling Longwave Radiation	rlds_tavg-u-hxy-u	W m^{-2}	3	monthly
rsus	Surface Upwelling	rsus_tavg-u-hxy-u	W m^{-2}	3	monthly

	Shortwave Radiation				
rlus	Surface Upwelling Longwave Radiation	rlus_tavg-u-hxy-u	W m^{-2}	3	monthly
hfls	Surface Upward Latent Heat Flux	hfls_tavg-u-hxy-u	W m^{-2}	3	monthly
hfss	Surface Upward Sensible Heat Flux	hfss_tavg-u-hxy-u	W m^{-2}	3	monthly
hfds	Downward Heat Flux at Sea Water Surface	hfds_tavg-u-hxy-sea	W m^{-2}	3	monthly
hfdsl	Ground heat flux	hfdsl_tavg-u-hxy-lnd	W m^{-2}	3	3-hourly
rsdsdiff	Surface Diffuse Downwelling Shortwave Radiation	rsdsdiff_tavg-u-hxy-u	W m^{-2}	3	daily
snm	Surface Snow Melt	snm_tavg-u-hxy-lnd	kg m^{-2} s^{-1}	3	monthly
snd	Snow Depth	snd_tavg-u-hxy-lnd	m	3	monthly
snc	Snow Area Percentage	snc_tavg-u-hxy-lnd	%	3	monthly
snw	Surface Snow Amount	snw tavg-u-hxy-lnd	kg m^{-2}	3	monthly
Atmosphere					
pr	Precipitation	pr_tavg-u-hxy-u	kg m^{-2} s^{-1}	3	monthly
tas	Near-surface air temperature	tas_tavg-h2m-hxy-u	K	3	monthly
tasmax	Daily Maximum Near-Surface Air Temperature	tas_tmax-h2m-hxy-u	K	3	monthly
tasmin	Daily Minimum Near-Surface Air Temperature	tas_tmin-h2m-hxy-u	K	3	monthly
sfcWind	Near-Surface Wind Speed	sfcWind_tavg-h10m-hxy-u	m s^{-1}	3	monthly
hurs	Near-Surface Relative Humidity	hurs_tavg-h2m-hxy-u	%	3	monthly
psl	Sea Level Pressure	psl_tavg-u-hxy-u	Pa	3	monthly
zg	Geopotential Height	zg_tavg-p19-hxy-air	m	4	monthly
ua	Eastward Wind	ua_tavg-p19-hxy-air	m s^{-1}	4	monthly
va	Northward Wind	va_tavg-p19-hxy-air	m s^{-1}	4	monthly
ta	Air Temperature	ta_tavg-p19-hxy-air	K	4	monthly
hus	Specific Humidity	hus_tavg-p19-hxy-u	1	4	monthly
cldnvi	Column Integrated Cloud Droplet Number	cldnvi_tavg-u-hxy-u	m^{-2}	3	monthly
clt	Total Cloud Cover Percentage	clt_tavg-u-hxy-u	%	3	monthly
rsdt	TOA Incident Shortwave Radiation	rsdt_tavg-u-hxy-u	W m^{-2}	3	monthly
rsdcs	Downwelling Clear-Sky Shortwave Radiation at the surface and TOA	rsdcs_tavg-alh-hxy-u	W m^{-2}	4	monthly

loadbc	Load of BC	loadbc_tavg-u-hxy-u	kg m-2	3	daily
loadpoa	Load of Dry Aerosol Primary Organic Matter	loadpoa_tavg-u-hxy-u	kg m^{-2}	3	daily
loadso4	Load of SO4	loadso4_tavg-u-hxy-u	kg m^{-2}	3	monthly
od550bb	Aerosol Optical Depth at 550nm Due to Biomass Burning	od550bb_tavg-u-hxy-u	1	3	monthly
od550bc	Black Carbon Optical Thickness at 550nm	od550bc_tavg-u-hxy-u	1	3	monthly
od550oa	Total Organic Aerosol Optical Depth at 550nm	od550oa_tavg-u-hxy-u	1	3	monthly
lwp	Liquid Water Path	lwp_tavg-u-hxy-u	kg m^{-2}	3	monthly
sfo3	O3 Volume Mixing Ratio in Lowest Model Layer	o3_tavg-h2m-hxy-u	mol mol^{-1}	3	hourly
sfpm25	PM2.5 Mass Mixing Ratio in Lowest Model Layer	sfpm25_tavg-h2m-hxy-u	kg kg^{-1}	3	daily
emico	Total Emission Rate of CO	emico_tavg-u-hxy-u	kg m^{-2} s^{-1}	3	monthly
emibbch4	total emission of CH4 from all biomass burning	emibbch4_tavg-u-hxy-u	kg m^{-2} s^{-1}	3	monthly
emich4	Total Emission Rate of CH_4	emich4_tavg-u-hxy-u	kg m^{-2} s^{-1}	3	monthly
ch4global	Global Mean Mole Fraction of CH4	ch4_tavg-u-hm-u	1E-09	1	monthly
eminox	Total Emission Rate of NO_X	eminox_tavg-u-hxy-u	kg m^{-2} s^{-1}	3	monthly
emibvoc	Total Emission Rate of Biogenic NMVOC	emibvoc_tavg-u-hxy-u	kg m^{-2} s^{-1}	3	monthly
emidust	Total Emission Rate of Dust	emidust_tavg-u-hxy-u	kg m^{-2} s^{-1}	3	monthly
Ocean and sea ice					
no3	Dissolved Nitrate Concentration	no3_tavg-ol-hxy-sea	mol m^{-3}	3	monthly
po4	Total Dissolved Inorganic Phosphorus Concentration	po4_tavg-ol-hxy-sea	mol m^{-3}	3	monthly
chl	Mass Concentration of Phytoplankton Expressed as Chlorophyll in Sea Water	chl_tavg-ol-hxy-sea	kg m^{-3}	3	monthly
talk	Total Alkalinity	talk_tavg-ol-hxy-sea	mol m^{-3}	3	monthly
fsfe	Surface Downward Net Flux of Iron	fsfe_tavg-u-hxy-sea	mol $m^{-2}s^{-1}$	3	monthly
dfe	Dissolved Iron Concentration	dfe_tavg-ol-hxy-sea	mol m^{-3}	3	monthly

uo	Sea Water X Velocity	uo_tavg-ol-hxy-sea	m s^{-1}	4	monthly
vo	Sea Water Y Velocity	vo_tavg-ol-hxy-sea	m s^{-1}	4	monthly
thetao	Sea Water Potential Temperature	thetao_tavg-ol-hxy-sea	degC	4	monthly
so	Sea Water Salinity	so_tavg-ol-hxy-sea	$1E^{-03}$	4	monthly
tos	Sea Surface Temperature	tos_tavg-u-hxy-sea	ºC	3	monthly
zos	Sea Surface Height Above Geoid	zos_tavg-u-hxy-sea	m	3	monthly
mlotst	Ocean Mixed Layer Thickness	mlotst_tavg-u-hxy-sea	m	3	monthly
msftyz	Ocean Meridional Overturning Mass Stream Function	msftm_tavg-ol-hys-sea	kg s^{-1} or S_v	4	monthly
siconc	Sea-Ice Area Fraction	siconc_tavg-u-hxy-u	1	3	monthly
sithick	Sea-Ice Thickness	sithick_tavg-u-hxy-si	m	3	monthly

5. Recommended analyses

This section is organized into three subsections: Fire simulation evaluation (Sec. 5.1), Fire changes and drivers (Sec. 5.2), and Fire impacts (Sec. 5.3), which correspond to the three scientific questions. The subsections are linked: evaluation identifies key strengths and biases that inform and enhance (by supporting model choice and bias correction) the reliability of assessed fire changes and impacts, while fire drivers and fire impacts are often connected by feedbacks, and can help diagnose bias sources in simulated fire-related variables (Fig. 1). This section outlines a minimal set of recommended CMIP7 FireMIP analyses, along with general methodological guidance and key considerations. Further methodological choices and additional analyses are expected to emerge from community-led studies using the openly available CMIP7 FireMIP outputs.

5.1 Fire simulation evaluation

Target variables and experiments: Burned-area fraction and fire carbon emissions (and fire trace gas and aerosol emissions for ESMs with interactive fire emissions) from the historical/esm-historical experiment. To attribute improvements or biases in fire simulations to atmospheric versus land-surface simulations, we recommend complementing the coupled-model evaluation with offline land-model simulations (e.g., FireMIP experiments outside CMIP and/or land-hist in CMIP7).

Evaluation metrics: The ability of CMIP7 ESMs to simulate global and regional total burned area

and fire emissions will be evaluated, as well as their spatial and temporal variability (including spatial pattern, recent and long-term historical trends, and phases of seasonal variability, magnitude of interannual and decadal variability), extreme fire frequency, and relationships between fires with climatic and socioeconomic factors (Fig. 1). Unlike offline simulations of land surface models and DGVMs, which are driven by observed climate data, coupled models in CMIP are free-running and driven solely by anthropogenic forcing. As a result, they are not designed to synchronize with the actual climate state of specific years or decades. Consequently, expecting a one-to-one match between CMIP-simulated and observed fires for any given year or decade is unrealistic. Instead, we recommend evaluating how fires respond to large-scale climate oscillations, such as ENSO and PDO for tropical fires, and AO/NAO for Arctic-boreal fires (Ward et al., 2016; Chen et al., 2017; Kim et al., 2020; Zhao et al., 2022; Li et al., 2024a).

The definitions of "extreme fire" should be applied consistently across models for inter-model comparison. Two percentile-based definitions that can be applied consistently across CMIP7 ESMs: (1) pool all values of a fire metric (e.g., annual, fire-season, or peak-month burned area fraction) within a given region/biome over a common reference period; define extremes as the top X% of this pooled distribution; then compute, at each grid cell, the fraction of years/seasons/months exceeding this threshold; (2) apply percentile thresholds at the grid-cell level, but only for grid cells that exceed a minimum annual burned-area-fraction threshold, to avoid defining extremes in locations with negligible burned area. One could conduct sensitivity tests to assess how inter-model conclusions depend on the chosen definition. To reduce the influence of spatial resolution, we suggest regridding model outputs and benchmarks to a common grid (e.g., 1º) before evaluations. To enable process-level diagnosis (beyond quantifying model–observation differences), we suggest interpreting these outcome metrics together with driver–response diagnostics that relate fire to key controls, including climate conditions, fuel availability/biomass, and socio-economic influences. Robust attribution further requires documenting key differences in fire parameterizations across ESMs.

Evaluation focus (CMIP6 limitations): To assess whether CMIP7 addresses the deficiencies identified in CMIP6 fire simulations, we will place particular emphasis on (i) recent trends in burned area, (ii) fire seasonality in the Northern midlatitudes, and (iii) the spatial and temporal variability of burned area and fire carbon emissions in the Arctic–boreal zone.

Key regions: Africa, the Amazon, and the Arctic-boreal zone. Africa accounts for more than half of global burned area. Fires in the Amazon and the Arctic–boreal zone are linked to potential tipping elements (Amazon rainforest dieback, boreal forest dieback, and permafrost thaw) and can undermine forest-based climate solutions, including afforestation/reforestation and boreal peatland rewetting.

Benchmarks (present day): Given the large uncertainties in global fire observations (Table 7; Li et al., 2024a; Kaiser et al., 2025), we recommend evaluating fire simulations against multiple benchmarks. For present-day burned area, benchmarks could include GFED5 (van der Werf et al., 2025), FireCCI5.1 (Chuvieco et al., 2019), FireCCI60 (Pettinari et al., 2025), and MODIS Collection 6.1 (Giglio et al., 2018). For present-day fire emissions, options include GFED5 (van der Werf et al., 2025), CAMS-GFAS1.2 (Kaiser et al., 2012), GFAS4HTAP (Kaiser et al., 2024; 2025), FINN2.5 (Wiedinmyer et al., 2023), FEER1 (Ichoku and Ellison, 2014), and QFED2.5 (Darmenov and da Silva, 2015). To reduce the influence of large uncertainties in fire observations, we suggest the following evaluation strategy. For global and regional totals, a simulation is considered reasonable if it falls within the spread across available benchmarks (e.g., the full benchmark range or the multi-benchmark mean ± 1 standard deviation). For temporal variability (seasonal to decadal) and long-term trends, we recommend evaluating variabilities or changes normalized by the corresponding global or regional mean/total. For spatial patterns, we suggest spatial (pattern) correlation between simulations and each benchmark; simulations are considered skillful if the correlation is statistically significant ($P<0.05$) for at least one benchmark, with smaller P and higher correlation with more benchmarks indicating better performance.

Benchmarks (long-term historical trend): We suggest using charcoal-based regional data from the Reading Palaeofire Database (RPD), which is based on records from 1480 sites (Harrison et al., 2022). Also, multi-source merged global gridded fire emission products, such as BB4CMIP5 (Lamarque et al., 2010), BB4CMIP6 (van Marle et al., 2017), and BB4CMIP7 (van Marle and van der Werf, 2025), as well as reconstructed global historical gridded burned area products from Guo et al. (2025) and FireCCILT11 (Otón et al., 2021) can be used for comparison with simulations, but they may include larger uncertainties than present-day satellite-based products and RPD.

Benchmarks (regional): Regional fire field observations may also serve as valuable benchmarks, e.g., National Interagency Fire Center (NIFC) historical wildfire statistics and Fire Program Analysis Fire-Occurrence Database (FPA FOD) for USA, Canadian National Fire Database (CNFDB), National

Forestry and Grassland Administration (NFGA) / Ministry of Emergency Management (MEM) annual wildfire statistics and bulletins for China. The above products are recommended but not limited to these.

Table 7. Summary description of satellite-based products as benchmarks for fire simulations

Name	Methods	Resolution	Period	Global total	reference
		Burned Area			
GFED5	MODIS BA & MODIS、ATSR、VIIRS active fire counts	0.25º monthly	1997−2022	802 Mha yr^{-1} [a]	Chen et al. (2023)
FireCCI5.1	MODIS reflectance &active fire counts	0.25º monthly	2001−2020	473 Mha yr^{-1} [a]	Chuvieco et al. (2019)
FireCCI6	MODIS & Sentinel-3 reflectance; MODIS & VIIRS active fire counts	0.25º monthly	2003−2024	634 Mha yr^{-1} [b]	Pettinari et al. (2025)
MODIS C6.1	MODIS reflectance &active fire counts	0.25º monthly	2001−present	430 Mha yr^{-1} [a]	Giglio et al. (2018)
		Fire emissions			
GFED5	fuel consumption, GFED5 burned area	0.25º monthly	1997−2022	3.4 Pg C yr^{-1} [c] 0.53 Pg CO yr^{-1} [c]	van der Werf et al. (2025)
CAMS-GFAS1.2	(GFED), MODIS FRP (GFAS), MODIS active	0.1º daily	2003−present	2.1 Pg C yr^{-1} [a] 0.36 Pg CO yr^{-1} [a]	Kaiser et al. (2012)
GFAS4HTAP1.2	fire counts (FINN), emis. Factor	0.1º daily	2003−2023	0.36 Pg CO yr^{-1} [d]	Kaiser et al. (2024)
FINN2.5		1km daily	2002−2023	0.58 Pg CO yr^{-1} [d]	Wiedinmyer et al. (2023)
FEER1	GFAS1.2 FRP & MODIS AOD	0.1º monthly	2003-2013	3.9 Pg C yr^{-1} [a] 0.56 Pg CO yr^{-1} [e]	Ichoku and Ellison (2014)
QFED2.5	MODIS & VIIRS FRP &MODIS AOD emis. factor	0.1º daily	2000-present	0.32 Pg CO yr^{-1} [e]	Darmenov and da Silva (2015)

[a] 2003−2014 average from Li et al. (2024); [b] 2003−2018 average from Pettinari et al. (2025); [c] 2003−2014 average from https://www.globalfiredata.org/; [d] 2003−2014 average from Kaiser et al. (2025); [e] 2012−2019 average from Wiedinmyer et al. (2023)

5.2 Fire changes and drivers

Fire changes: We recommend quantifying past, present, and future fire changes using burned area (burntFractionAll) and fire carbon emissions (fFire) from historical/esm-historical and ScenarioMIP experiments (Table 1). These changes include, but are not limited to, changes in annual totals, seasonality

(timing of fire-season onset and end, fire-season length, peak activity), frequency of extremes, and interannual variation.

Uncertainties in simulated fire changes: CMIP7 FireMIP will provide multi-model, multi-initial-condition, and multi-scenario ensembles. These ensembles provide an opportunity to quantify total uncertainty in simulated fire changes and to partition it into contributions from model uncertainty, initial-condition (internal-variability) uncertainty, and scenario uncertainty.

Fire drivers and causal pathways: Fires are regulated by multiple local, direct drivers that can be grouped into three categories: ecosystem, climate, and socio-economic factors (Fig. 1). Ecosystem factors include aboveground biomass, which sets the fuel load. Climate factors include air humidity, soil moisture, and/or precipitation, which determine fuel wetness, and wind speed, which affects the fire spread rate and indirectly influences fuel wetness. Socio-economic factors include population density, GDP, and land use, which (as ESM forcing data) affect human ignitions and fire suppressions. By comparing hist-nat, hist-aer, hist-GHG, and hist-lu with historical/esm-historical, the effects of natural forcing, anthropogenic forcing, as well as anthropogenic aerosols, greenhouse gases, and land-use changes on local variables and fires can be quantified, and the pathways across Earth system components can be analyzed (Fig. 1). For example, in the Arctic–boreal zone, increasing anthropogenic GHG lead to warming, which can accelerate permafrost thaw and soil drying, thereby drying fuels and increasing fire risks, inferred from mechanisms described in Kim et al. (2024) and Cai (2024). Comparing the influences of different forcings helps identify the dominant one and pathway.

5.3 Fire impacts

Impacts of fire and fire aerosols (historical): The influence of fire and fire aerosol emissions can be quantified by comparing outputs from the historical/esm-historical simulations with those from hist-no-fire and hist-no-fireaero, respectively. Specifically, analyses will focus on variables in eight categories: (i) the land–atmosphere–ocean coupled carbon, water, and energy cycles; (ii) vegetation composition and structure; (iii) fire-induced trace gas and aerosol emissions; (iv) atmospheric responses, including atmospheric circulation, composition, and chemistry; (v) surface climate (e.g., temperature, humidity, precipitation, and wind speed); (vi) cryosphere conditions (e.g., permafrost extent and active-layer thickness, snow and sea-ice extent and depth); (vii) ocean responses, including ocean physics (currents, temperature, salinity) and marine ecosystems; and (viii) human health impacts, based on simulated

surface $PM_{2.5}$ or O_3 concentrations in ESMs, or estimated outside ESMs using simulated fire carbon emissions and atmospheric (chemistry) models. We additionally recommend stratifying analyses by model configuration (prescribed versus interactive fire emissions) to assess the sensitivity of inferred fire impacts; consistent results across configurations would increase confidence, whereas discrepancies would motivate further investigation.

Impacts of changes in fire and fire aerosols (future): The influence of future fire and fire aerosol emission changes could be quantified using scen7-h compared against scen7-h-no-firechange and scen7-h-no-fireaerochange, respectively, with analyses of a similar variable set. Related uncertainties can also be assessed using multi-model and multi-initial-condition ensemble members.

Underlying mechanisms: By quantifying changes in key variables along different pathways and comparing them, the dominant pathway through which fire exerts a statistically significant influence on the target variables can be identified. For example, CESM-based estimates show that fire aerosol emissions can affect global precipitation through two pathways: (1) increasing cloud droplet number concentration and thus increasing cloud water path, which tends to reduce precipitation; and (2) fire-aerosol-induced cooling that lowers evaporation and reduces atmospheric water vapor, which also tends to reduce precipitation. Our results show that the reduction in atmospheric water vapor is much stronger than the increase in cloud water, indicating that the second pathway is dominant (Fig. 8a in Li et al., 2022).

Benefits of the coupled CMIP7 framework: The full output dataset will support building the first comprehensive picture of global fire's role in the land–atmosphere–ocean carbon cycle. It will also allow for more accurate and reliable quantification of fire impacts on global and regional climate, benefiting from CMIP7 coupling simulations that incorporate aerosol-cloud interaction modeling, fully coupled ocean models rather than prescribed SSTs or slab ocean models, and multi-model, multi-initial-condition ensembles.

6 Summary

This paper outlines the protocol for CMIP7 FireMIP, detailing its motivation, experimental design, model inputs and outputs, and recommended analyses.

Previous FireMIP studies provided valuable insights into fire's local drivers and local impacts on vegetation and land carbon dynamics using DGVMs but were limited by offline approaches that could

not capture fire-climate and ecosystem-climate interactions. Earlier coupled-model studies lacked either critical climate feedback and processes necessary for accurately quantifying fire impacts or an ensemble framework to support comprehensive uncertainty assessment.

FireMIP's integration into CMIP7 aims to address these limitations by using fully coupled ESMs and a multi-model, multi-initial-condition, and multi-scenario ensemble framework. This allows for a systematic assessment of fire regime changes and fire's interactions with the biosphere, land, atmosphere, hydrosphere, cryosphere, and human systems. By capturing fire response and feedbacks across Earth system components, both local and remote, contemporary and legacy, FireMIP in CMIP7 will provide a more comprehensive understanding of fire's role in the Earth system and improve the scientific basis for fire and environmental management and climate-change mitigation.

CMIP7 aims to answer four science questions: (1) patterns of sea surface change; (2) changing dangerous weather; (3) the water-carbon-climate nexus; and (4) tipping points (Dunne et al., 2025). As the only fire-focused MIP in CMIP7, FireMIP relates to questions (1) and (2) and will help address questions (3) and (4). First, FireMIP can assess how fire-driven aerosol forcing and land–atmosphere flux changes influence large-scale atmospheric circulation and subsequently SST patterns. Second, because fires are closely linked to drought and heatwaves, FireMIP's analysis of fire-regime changes can inform how the associated hazards of changing dangerous weather may evolve. Third, because fire is an integral process linking water, carbon, and climate, FireMIP's assessment of fire drivers and impacts can help clarify interactions among them and inform how the water–carbon–climate nexus may respond to anthropogenic forcings. In addition, fires interact with systems that exhibit tipping-point behavior, such as the Amazon rainforests, boreal forests, permafrost, and Arctic sea ice, so FireMIP can help identify fire-related pathways that may increase the likelihood of abrupt or irreversible transitions.

Updated details on the project and its progress will be available at https://wcrp-cmip.org/mips/firemip/ (last access: 1 Oct 2025)

Code and Data availability.

The protocol paper does not include any code or datasets. The model output from the CMIP7 FireMIP simulations will be distributed through the Earth System Grid Federation (ESGF) and will be freely accessible through ESGF data portals after registration, following standard CMIP7 formats, consistent with other MIPs within CMIP7.

Author contribution.

FL wrote and revised the paper. FL, DL, VKA, BR, HH, MK, RL, ZL, DW, and VA designed the experiments, and FL, YJ, AW, and YL selected the output variables. CL assisted FL in preparing the tables and formatting the reference list. All authors reviewed and edited the paper.

Acknowledgements.

We appreciate the helpful discussions and suggestions on experimental design and output variables from Vivek K. Arora, Keren Mezuman, Jiawen Zhu, Jin-Soo Kim, Zhongwang Wei, Lei Cai, Guangqing Zhou, Maria Val Martin, Kece Fei, Eleanor O'Rourke, Elisabeth Dingley, Yang Chen, Peter Lawrence, Sam Rabin, Simone Tilmes, Lili Xia, Kazuhisa Tanada, Ian Eisenman, Meinrat O. Andreae, Jong-Seong Kug, Xu Yue, Zehao Shen, Hailong Liu, Pengfei Lin, Yiran Peng, Yong Wang, and Xiaodong Zeng. We thank the editor, Tatiana Egorova, for her time and efforts in facilitating the review process, as well as the two reviewers for their positive assessment and constructive comments. We also thank the CMIP International Project Office (IPO) for supporting FireMIP, the CMIP Climate Forcings Task Team and input4MIPs for providing CMIP7 forcing data for the experiments, and ESGF for facilitating the distribution of FireMIP experiment outputs.

Financial Supports.

This study is co-supported by the National Key Research and Development Program of China (grant nos. 2022YFE0106500 and 2024YFF0809000), the Guangdong Major Project of Basic and Applied Basic Research (grant no. 2021B0301030007), and the National Science and Technology Infrastructure project Earth System Science Numerical Simulator Facility (EarthLab). DML is supported by the NSF National Center for Atmospheric Research, which is a major facility sponsored by the U.S. National Science Foundation under Cooperative Agreement No. 1852977. BMR was supported by Google.org and funding catalyzed by the TED Audacious Project (Permafrost Pathways). CB was supported by the Met Office Hadley Centre Climate Programme funded by DSIT, and the Met Office Climate Science for Service Partnership (CSSP) Brazil project under the International Science Partnerships Fund (ISPF). HL was supported by the Research Council of Norway project (328922). RL was supported by the Office of Science, U.S. Department of Energy, Biological and Environmental

Research as part of the Earth and Environmental Systems Modeling (EESM) Program. PNNL is operated for the U.S. DOE by Battelle Memorial Institute for DOE under contract AC05-76RL01830. MK and AV were supported by the Leverhulme Trust through the Leverhulme Centre for Wildfires, Environment and Society, grant number RC-2018-023. AV has also been supported by the AXA Research Fund (project 'AXA Chair in Wildfires and Climate', CPO00163217), by the Hellenic Foundation for Research and Innovation (grants FirePC and REINFORCE, with Grant IDs 3453 and 15155, respectively), and by the Horizon Europe programme under Grant Agreement No. 101137680 via project CERTAINTY.

Competing interests.

One author (David M. Lawrence) is a member of the editorial board of GMD.

References

Andela, N., Morton, D. C., Giglio, L., Chen, Y., van der Werf, G. R., Kasibhatla, P. S., DeFries, R. S., Collatz, G. J., Hantson, S., Kloster, S., Bachelet, D., Forrest, M., Lasslop, G., Li, F., Mangeon, S., Melton, J. R., Yue, C., and Randerson, J. T.: A human-driven decline in global burned area, Science, 356, 1356–1362, https://doi.org/10.1126/science.aal4108, 2017.

Arora, V. K. and Melton, J. R.: Reduction in global area burned and wildfire emissions since 1930s enhances carbon uptake by land, Nat. Commun., 9, 1326, https://doi.org/10.1038/s41467-018-03838-0, 2018.

Beaudor, M., Pouyaei, A., and Wang, R.: How Could Fire Emissions Reshape the Nitrogen Cycle?, Geophys. Res. Lett., published 20 Nov 2025, https://doi.org/10.1029/2025GL116250.

Bhattarai, H., Val Martin, M., Sitch, S., Yung, D. H. Y., and Tai, A. P. K.: Global patterns and drivers of climate-driven fires in a warming world, EGUsphere [preprint], https://doi.org/10.5194/egusphere-2025-804, 2025.

Bond-Lamberty, B., Peckham, S. D., Ahl, D. E., and Gower, S. T.: Fire as the dominant driver of central Canadian boreal forest carbon balance, Nature, 450, 89–92, https://doi.org/10.1038/nature06272, 2007.

Boysen, L. R., Brovkin, V., Pongratz, J., Lawrence, D. M., Lawrence, P., Vuichard, N., Peylin, P., Liddicoat, S., Hajima, T., Zhang, Y., Rocher, M., Delire, C., Séférian, R., Arora, V. K., Nieradzik, L., Anthoni, P., Thiery, W., Laguë, M. M., Lawrence, D., and Lo, M.-H.: Global climate response to idealized deforestation in CMIP6 models, Biogeosciences, 17, 5615–5638, https://doi.org/10.5194/bg-17-5615-2020, 2020.

Bowman, D. M. J. S., Balch, J. K., Artaxo, P., Bond, W. J., Carlson, J. M., Cochrane, M. A., D'Antonio, C. M., DeFries, R. S., Doyle, J. C., Harrison, S. P., Johnston, F. H., Keeley, J. E., Krawchuk, M. A., Kull, C. A., Marston, J. B., Moritz, M. A., Prentice, I. C., Roos, C. I., Scott, A. C., Swetnam, T. W., van der Werf, G. R., and Pyne, S. J.: Fire in the Earth system, Science, 324, 481–484, https://doi.org/10.1126/science.1163886, 2009.

Burton, C., Lampe, S., Kelley, D. I., Thiery, W., Hantson, S., Christidis, N., Gudmundsson, L., Forrest, M., Burke, E., Chang, J., Huang, H., Ito, A., Kou-Giesbrecht, S., Lasslop, G., Li, W., Nieradzik, L., Li, F., Chen, Y., Randerson, J., Reyer, C. P. O., and Mengel, M.: Global burned area increasingly explained by climate change, Nat. Clim. Change, 14, 1186–1192, https://doi.org/10.1038/s41558-024-02140-w, 2024.

Cai, L., Permafrost thaw as a critical driver of naturally-ignited wildfires in the high latitudes, Workshop: Response and Feedback of Arctic-boreal Permafrost and Wildfires to Climate Change, Beijing, Oct 9–11, 2024.

Chen, Y., Morton, D. C., Andela, N., van der Werf, G. R., Giglio, L., and Randerson, J. T.: A pan-tropical cascade of fire driven by El Niño/Southern Oscillation, Nat. Clim. Chang., 7, 906–911, https://doi.org/10.1038/s41558-017-0014-8, 2017.

Chen, Y., Romps, D. M., Seeley, J. T., Veraverbeke, S., Riley, W. J., Mekonnen, Z. A., Randerson, J. T.: Future increases in Arctic lightning and fire risk for permafrost carbon, Nat. Clim. Chang., 11, 404–410, https://doi.org/10.1038/s41558-021-01011-y, 2021.

Chen, Y., Hall, J., van Wees, D., Andela, N., Hantson, S., Giglio, L., van der Werf, G. R., Morton, D. C., and Randerson, J. T.: Multi-decadal trends and variability in burned area from the fifth version of the Global Fire Emissions Database (GFED5), Earth Syst. Sci. Data, 15, 5227–5259, https://doi.org/10.5194/essd-15-5227-2023, 2023.

Chuvieco, E., Mouillot, F., van der Werf, G. R., San Miguel, J., Tanasse, M., Koutsias, N., García, M., Yebra, M., Padilla, M., Gitas, I., Heili, A., Hawbaker, T. J., and Giglio, L.: Historical background and current developments for mapping burned area from satellite Earth observation, Remote Sens. Environ., 225, 45–64, https://doi.org/10.1016/j.rse.2019.02.013, 2019.

Cunningham, C. X., Abatzoglou, J. T., Kolden, C. A., Williamson, G. J., Steuer, M., Bowman, D. M. J. S.: Climate-linked escalation of societally disastrous wildfires, Science, 390, 53–58, https://doi.org/10.1126/science.adr5127, 2025.

Darmenov, A. and da Silva, A.: The Quick Fire Emissions Dataset (QFED): Documentation of versions 2.1, 2.2 and 2.4, NASA Technical Report Series on Global Modeling and Data Assimilation, NASA TM-2015-104606, Volume 38, http://gmao.gsfc.nasa.gov/pubs/docs/Darmenov796.pdf, 2015.

Dunne, J. P., Hewitt, H. T., Arblaster, J. M., Bonou, F., Boucher, O., Cavazos, T., Dingley, B., Durack, P. J., Hassler, B., Juckes, M., Miyakawa, T., Mizielinski, M., Naik, V., Nicholls, Z., O'Rourke, E., Pincus, R., Sanderson, B. M., Simpson, I. R., and Taylor, K. E.: An evolving Coupled Model Intercomparison Project phase 7 (CMIP7) and Fast Track in support of future climate assessment, Geosci. Model Dev., 18, 6671–6700, https://doi.org/10.5194/gmd-18-6671-2025, 2025.

Frieler, K., Volkholz, J., Lange, S., Schewe, J., Mengel, M., del Rocío Rivas López, M., Otto, C., Reyer, C. P. O., Karger, D. N., Malle, J. T., Treu, S., Menz, C., Blanchard, J. L., Harrison, C. S., Petrik, C. M., Eddy, T. D., Ortega-Cisneros, K., Novaglio, C., Rousseau, Y., Watson, R. A., Stock, C., Liu, X., Heneghan, R., Tittensor, D., Maury, O., Büchner, M., Vogt, T., Wang, T., Sun, F., Sauer, I. J., Koch, J., Vanderkelen, I., Jägermeyr, J., Müller, C., Rabin, S., Klar, J., Vega del Valle, I. D., Lasslop, G., Chadburn, S., Burke, E., Gallego-Sala, A., Smith, N., Chang, J., Hantson, S.,

Burton, C., Gädeke, A., Li, F., Gosling, S. N., Müller Schmied, H., Hattermann, F., Wang, J., Yao, F., Hickler, T., Marcé, R., Pierson, D., Thiery, W., Mercado-Bettín, D., Ladwig, R., Ayala-Zamora, A. I., Forrest, M., and Bechtold, M.: Scenario setup and forcing data for impact model evaluation and impact attribution within the third round of the Inter-Sectoral Impact Model Intercomparison Project (ISIMIP3a), Geosci. Model Dev., 17, 1–51, https://doi.org/10.5194/gmd-17-1-2024, 2024.

Giglio, L., Boschetti, L., Roy, D. P., Humber, M. L., and Justice, C. O.: The Collection 6 MODIS burned area mapping algorithm and product, Remote Sens. Environ., 217, 72–85, https://doi.org/10.1016/j.rse.2018.08.005, 2018.

Gillett, N. P., Simpson, I. R., Hegerl, G., Knutti, R., Mitchell, D., Ribes, A., Shiogama, H., Stone, D., Tebaldi, C., Wolski, P., Zhang, W., and Arora, V. K.: The Detection and Attribution Model Intercomparison Project (DAMIP v2.0) contribution to CMIP7, Geosci. Model Dev., 18, 4399–4416, https://doi.org/10.5194/gmd-18-4399-2025, 2025.

Grandey, B. S., Lee, H.-H., and Wang, C.: Radiative effects of interannually varying vs. interannually invariant aerosol emissions from fires, Atmos. Chem. Phys., 16, 14495–14513, https://doi.org/10.5194/acp-16-14495-2016, 2016.

Guo, Z., Li, W., Ciais, P., Sitch, S., van der Werf, G. R., Bowring, S. P. K., Bastos, A., Mouillot, F., He, J., Sun, M., Zhu, L., Du, X., Wang, N., and Huang, X.: Reconstructed global monthly burned area maps from 1901 to 2020, Earth Syst. Sci. Data, 17, 3599–3618, https://doi.org/10.5194/essd-17-3599-2025, 2025.

Hamilton, D., Wan, J., Liguori-Bills, N., Kasoar, M., and Hantson, S.: Past and Future Fire Emission Trajectories & Aerosol Radiative Forcing, WCRP-CMIP, https://wcrp-cmip.org/wp-content/uploads/2024/10/S4_DHamilton_TO-PUBLISH.pdf, 2024.

Hantson, S., Arneth, A., Harrison, S. P., Kelley, D. I., Prentice, I. C., Rabin, S. S., Archibald, S., Mouillot, F., Arnold, S. R., Artaxo, P., Bachelet, D., Ciais, P., Forrest, M., Friedlingstein, P., Hickler, T., Kaplan, J. O., Kloster, S., Knorr, W., Lasslop, G., Li, F., Mangeon, S., Melton, J. R., Meyn, A., Sitch, S., Spessa, A., van der Werf, G. R., Voulgarakis, A., and Yue, C.: The status and challenge of global fire modelling, Biogeosciences, 13, 3359–3375, https://doi.org/10.5194/bg-13-3359-2016, 2016.

Harrison, S. P., Villegas-Diaz, R., Cruz-Silva, E., Gallagher, D., Kesner, D., Lincoln, P., Shen, Y., Sweeney, L., Colombaroli, D., Ali, A., Barhoumi, C., Bergeron, Y., Blyakharchuk, T., Bobek, P., Bradshaw, R., Clear, J. L., Czerwiński, S., Daniau, A.-L., Dodson, J., Edwards, K. J., Edwards, M. E., Feurdean, A., Foster, D., Gajewski, K., Gałka, M., Garneau, M., Giesecke, T., Gil Romera, G., Girardin, M. P., Hoefer, D., Huang, K., Inoue, J., Jamrichová, E., Jasiunas, N., Jiang, W., Jiménez-Moreno, G., Karpińska-Kołaczek, M., Kołaczek, P., Kuosmanen, N., Lamentowicz, M., Lavoie, M., Li, F., Li, J., Lisitsyna, O., López-Sáez, J. A., Luelmo-Lautenschlaeger, R., Magnan, G., Magyari, E. K., Maksims, A., Marcisz, K., Marinova, E., Marlon, J., Mensing, S., Miroslaw-Grabowska, J., Oswald, W., Pérez-Díaz, S., Pérez-Obiol, R., Piilo, S., Poska, A., Qin, X., Remy, C. C., Richard, P. J. H., Salonen, S., Sasaki, N., Schneider, H., Shotyk, W., Stancikaite, M., Šteinberga, D., Stivrins, N., Takahara, H., Tan, Z., Trasune, L., Umbanhowar, C. E., Väliranta, M., Vassiljev, J., Xiao, X., Xu, Q., Xu, X., Zawisza, E., Zhao, Y., Zhou, Z., and Paillard, J.: The

Reading Palaeofire Database: an expanded global resource to document changes in fire regimes from sedimentary charcoal records, Earth Syst. Sci. Data, 14, 1109–1124, https://doi.org/10.5194/essd-14-1109-2022, 2022.

Harrison, S. P., Haas, O., Bartlein, P. J., Sweeney, L., and Zhang, G.: Climate, vegetation, people: disentangling the controls of fire at different timescales, Phil. Trans. R. Soc. B, 380, 20230464, https://doi.org/10.1098/rstb.2023.0464, 2025.

Ichoku, C. and Ellison, L.: Global top-down smoke-aerosol emissions estimation using satellite fire radiative power measurements, Atmos. Chem. Phys., 14, 6643–6667, https://doi.org/10.5194/acp-14-6643-2014, 2014.

IPCC: Climate Change 2021: The Physical Science Basis. Contribution of Working Group I to the Sixth Assessment Report of the Intergovernmental Panel on Climate Change, edited by: Masson-Delmotte, V., Zhai, P., Pirani, A., Connors, S. L., Péan, C., Berger, S., Caud, N., Chen, Y., Goldfarb, L., Gomis, M. I., Huang, M., Leitzell, K., Lonnoy, E., Matthews, J. B. R., Maycock, T. K., Waterfield, T., Yelekçi, O., Yu, R., and Zhou, B., Cambridge University Press, Cambridge, United Kingdom and New York, NY, USA, 2391 pp., 2021.

Jiang, Y., Lu, Z., Liu, X., Qian, Y., Zhang, K., Wang, Y., and Yang, X.-Q.: Impacts of global open-fire aerosols on direct radiative, cloud and surface-albedo effects simulated with CAM5, Atmos. Chem. Phys., 16, 14805–14824, https://doi.org/10.5194/acp-16-14805-2016, 2016.

Jiang, Y., Yang, X. Q., Liu, X., Qian, Y., Zhang, K., Wang, M., Li, F., Wang, Y., and Lu, Z.: Impacts of wildfire aerosols on global energy budget and climate: The role of climate feedbacks, J. Clim., 33, 3351–3366, https://doi.org/10.1175/JCLI-D-19-0572.1, 2020.

Jones, M. W., Abatzoglou, J. T., Veraverbeke, S., Andela, N., Lasslop, G., Forkel, M., Smith, A. J. P., Burton, C., Betts, R. A., van der Werf, G. R., Sitch, S., Canadell, J. G., Santín, C., Kolden, C., Doerr, S. H., and Le Q, C.: Global and regional trends and drivers of fire under climate change, Reviews of Geophysics, 60, e2020RG000726, https://doi.org/10.1029/2020RG000726, 2022.

Kaiser, J. W., Heil, A., Andreae, M. O., Benedetti, A., Chubarova, N., Jones, L., Morcrette, J.-J., Razinger, M., Schultz, M. G., Suttie, M., and van der Werf, G. R.: Biomass burning emissions estimated with a global fire assimilation system based on observed fire radiative power, Biogeosciences, 9, 527–554, https://doi.org/10.5194/bg-9-527-2012, 2012.

Kaiser, J., Huijnen, V., Remy, S., Ytre-Eide, M. A., De Jong, M. C., Zheng, B., and Wiedinmyer, C.: Evaluation of fire emissions for HTAP3 with CAMS GFAS and IFS-COMPO, EGU General Assembly 2025, Vienna, Austria, 27 Apr–2 May 2025, EGU25-8708, https://doi.org/10.5194/egusphere-egu25-8708, 2025.

Kaiser, J. and Holmedal, D. G.: GFAS4HTAPv1.2.1 vegetation fire emissions 2003-2023 (Beta), Zenodo [data set], https://doi.org/10.5281/zenodo.13753452, 2024.

Kay, J. E., Deser, C., Phillips, A., Mai, A., Hannay, C., Strand, G., Arblaster, J. M., Bates, S. C., Danabasoglu, G., Edwards, J., Holland, M., Kushner, P., Lamarque, J.-F., Lawrence, D., Lindsay, K., Middleton, A., Munoz, E., Neale, R., Oleson, K., Polvani, L., and Vertenstein, M.: The Community Earth System Model (CESM) Large Ensemble Project: a community resource for

studying climate change in the presence of internal climate variability, B. Am. Meteorol. Soc., 96, 1333–1349, https://doi.org/10.1175/bams-d-13-00255.1, 2015.

Kim, I.-W., Timmermann, A., Kim, J.-E., Rodgers, K. B., Lee, S.-S., Lee, H., and Wieder, W. R.: Abrupt increase in Arctic–Subarctic wildfires caused by future permafrost thaw, Nat. Commun., 15, 7868, https://doi.org/10.1038/s41467-024-51447-4, 2024.

Kim, J.-S., Kug, J.-S., Jeong, S.-J., Park, H., and Schaepman-Strub, G.: Extensive fires in southeastern Siberian permafrost linked to preceding Arctic Oscillation, Sci. Adv., 6, eaax3308, https://doi.org/10.1126/sciadv.aax3308, 2020.

Kloster, S. and Lasslop, G.: Historical and future fire occurrence (1850 to 2100) simulated in CMIP5 Earth System Models, Global Planet. Change, 150, 58–69, https://doi.org/10.1016/j.gloplacha.2016.12.017, 2017.

Lamarque, J.-F., Bond, T. C., Eyring, V., Granier, C., Heil, A., Klimont, Z., Lee, D., Liousse, C., Mieville, A., Owen, B., Schultz, M. G., Shindell, D., Smith, S. J., Stehfest, E., Van Aardenne, J., Cooper, O. R., Kainuma, M., Mahowald, N., McConnell, J. R., Naik, V., Riahi, K., and van Vuuren, D. P.: Historical (1850–2000) gridded anthropogenic and biomass burning emissions of reactive gases and aerosols: methodology and application, Atmos. Chem. Phys., 10, 7017–7039, https://doi.org/10.5194/acp-10-7017-2010, 2010.

Landry, J.-S., Partanen, A.-I., and Matthews, H. D.: Carbon cycle and climate effects of forcing from fire-emitted aerosols, Environ. Res. Lett, 12, 025002, https://doi.org/10.1088/1748-9326/aa51de, 2017.

Lasslop, G., Coppola, A. I., Voulgarakis, A., Yue, C., and Veraverbeke, S.: Influence of Fire on the Carbon Cycle and Climate, Curr. Clim. Change Rep., 5, 112–123, https://doi.org/10.1007/s40641-019-00128-9, 2019.

Lasslop, G., Hantson, S., Harrison, S. P., Bachelet, D., Burton, C., Forkel, M., Forrest, M., Li, F., Melton, J. R., Yue, C., Archibald, S., Scheiter, S., Arneth, A., Hickler, T., and Sitch, S.: Global ecosystems and fire: Multi-model assessment of fire-induced tree-cover and carbon storage reduction, Global Change Biology, 26, 5027–5041, https://doi.org/10.1111/gcb.15160, 2020.

Lenton, T. M., Rockström, J., Gaffney, O., Rahmstorf, S., Richardson, K., Steffen, W., and Schellnhuber, H. J.: Climate tipping points – too risky to bet against, Nature, 575, 592–595, https://doi.org/10.1038/d41586-019-03595-0, 2019.

Li, F.: Quantifying the impacts of fire aerosols on global terrestrial ecosystem productivity with the fully-coupled Earth system model CESM, Atmos. Oceanic Sci Lett, 13, 330–337, https://doi.org/10.1080/16742834.2020.1740580, 2020.

Li, F.: Fires in CMIP6 models, 2021 FireMIP workshop, Zoom, Nov 9, 2021.

Li, F., Bond-Lamberty, B., and Levis, S.: Quantifying the role of fire in the Earth system – Part 2: Impact on the net carbon balance of global terrestrial ecosystems for the 20th century, Biogeosciences, 11, 1345–1360, https://doi.org/10.5194/bg-11-1345-2014, 2014.

Li, F. and Lawrence, D. M.: Role of fire in the global land water budget during the 20th century through changing ecosystems, J. Clim., 30, 1893–1908, https://doi.org/10.1175/JCLI-D-16-0460.1, 2017a.

Li, Fang, Lawrence, D. M., Bond-Lamberty, B.: Human impacts on 20th century fire dynamics and implications for global carbon and water trajectories, Glob. Planet. Change, 162, 18-27, http://dx.doi.org/10.1016/j.gloplacha.2018.01.002, 2018.

Li, F., Lawrence, D. M., and Bond-Lamberty, B.: Impact of fire on global land surface air temperature and energy budget for the 20th century due to changes within ecosystems, Environ. Res. Lett, 12, 044014, https://doi.org/10.1088/1748-9326/aa6685, 2017b.

Li, F., Lawrence, D. M., Jiang, Y., Liu, X., and Lin, Z.: Fire aerosols slow down the global water cycle, J. Clim., 35, 3619–3633, https://doi.org/10.1175/JCLI-D-21-0245.1, 2022.

Li, F., Song, X., Harrison, S. P., Marlon, J. R., Lin, Z., Leung, L. R., Schwinger, J., Marécal, V., Wang, S., Ward, D. S., Dong, X., Lee, H., Nieradzik, L., Rabin, S. S., and Séférian, R.: Evaluation of global fire simulations in CMIP6 Earth system models, Geosci. Model Dev., 17, 8751–8771, https://doi.org/10.5194/gmd-17-8751-2024, 2024.

Li, F., Val Martin, M., Andreae, M. O., Arneth, A., Hantson, S., Kaiser, J. W., Lasslop, G., Yue, C., Bachelet, D., Forrest, M., Kluzek, E., Liu, X., Mangeon, S., Melton, J. R., Ward, D. S., Darmenov, A., Hickler, T., Ichoku, C., Magi, B. I., Sitch, S., van der Werf, G. R., Wiedinmyer, C., and Rabin, S. S.: Historical (1700–2012) global multi-model estimates of the fire emissions from the Fire Modeling Intercomparison Project (FireMIP), Atmos. Chem. Phys., 19, 12545–12567, https://doi.org/10.5194/acp-19-12545-2019, 2019.

Li, F., Levis, S., and Ward, D. S.: Quantifying the role of fire in the Earth system – Part 1: Improved global fire modeling in the Community Earth System Model (CESM1), Biogeosciences, 10, 2293–2314, https://doi.org/10.5194/bg-10-2293-2013, 2013.

Lizundia-Loiola, J., Franquesa, M., Khairoun, A., and Chuvieco, E.: Global burned area mapping from Sentinel-3 Synergy and VIIRS active fires, Remote Sens. Environ., 282, 113298, https://doi.org/10.1016/j.rse.2022.113298, 2022.

Lou, S., Liu, Y., Bai, Y., Li, F., Lin, G., Xu, L., Liu, Z., Chen, Y., Dong, X., Zhao, M., Wang, L., Jin, M., Wang, C., Cai, W., Gong, P., and Luo, Y.: Projections of mortality risk attributable to short-term exposure to landscape fire smoke in China, 2021–2100: A health impact assessment study, Lancet Planet. Heath, 7, e841–e849, https://doi.org/10.1016/S2542-5196(23)00192-4, 2023.

Mao, J: Fires jeopardize world's carbon sink, Nat. Geosci. 17, 1072–1073, https://doi.org/10.1038/s41561-024-01562-7, 2024.

Oberhagemann, L., Billing, M., von Bloh, W., Drüke, M., Forrest, M., Bowring, S. P. K., Hetzer, J., Ribalaygua Batalla, J., and Thonicke, K.: Sources of uncertainty in the SPITFIRE global fire model: development of LPJmL-SPITFIRE1.9 and directions for future improvements, Geosci. Model Dev., 18, 2021–2050, https://doi.org/10.5194/gmd-18-2021-2025, 2025.

Otón, G., Lizundia-Loiola, J., Pettinari, M. L., and Chuvieco, E.: Development of a consistent global long-term burned area product (1982–2018) based on AVHRR-LTDR data, Int. J. Appl. Earth Obs. Geoinf., 103, 102473, https://doi.org/10.1016/j.jag.2021.102473, 2021.

Park, C., Takahashi, K., Fujimori, S., Phung, V., Li, F., Takakura, J., Hasegawa, T., and Jansakoo, T.: Future fire-PM2.5 mortality varies depending on climate and socioeconomic changes, Environ. Res. Lett., 19, 024003, https://doi.org/10.1088/1748-9326/ad1b7d, 2024.

Pellegrini, A. F. A., Reich, P. B., Hobbie, S. E., Coetsee, C., Wigley, B., February, E., Georgiou, K., Terrer, C., Brookshire, E. N. J., and Ahlström, A.,: Soil carbon storage capacity of drylands under altered fire regimes, Nat. Clim. Chang., 13, 1089–1094, https://doi.org/10.1038/s41558-023-01800-7, 2023.

Pettinari, M. L., Khairoun, A., Torres-Vázquez, M. Á., Storm, T., Boettcher, M., and Chuvieco, E.: FireCCI Burned Area Algorithms and Products for Climate Modelling, Living Planet Symposium, Vienna, Austria, 23–27 June 2025.

Rabin, S. S., Melton, J. R., Lasslop, G., Bachelet, D., Forrest, M., Hantson, S., Kaplan, J. O., Li, F., Mangeon, S., Ward, D. S., Yue, C., Arora, V. K., Hickler, T., Kloster, S., Knorr, W., Nieradzik, L., Spessa, A., Folberth, G. A., Sheehan, T., Voulgarakis, A., Kelley, D. I., Prentice, I. C., Sitch, S., Harrison, S., and Arneth, A.: The Fire Modeling Intercomparison Project (FireMIP), phase 1: experimental and analytical protocols with detailed model descriptions, Geosci. Model Dev., 10, 1175–1197, https://doi.org/10.5194/gmd-10-1175-2017, 2017.

Randerson, J. T., Liu, H., Flanner, M. G., Chambers, S. D., Jin, Y., Hess, P. G., Pfister, G., Mack, M. C., Treseder, K. K., Welp, L. R., and Chapin, F. S.: The impact of boreal forest fire on climate warming, Science, 314, 1130–1132, https://doi.org/10.1126/science.1132075, 2006.

Sayedi, S. S., Abbott, B. W., Vannière, B., Leys, B., Colombaroli, D., Romera, G. G., Słowiński, M., Aleman, J. C., Blarquez, O., Feurdean, A., and Brown, K.: Assessing changes in global fire regimes, Fire Ecol., 20, 18, https://doi.org/10.1186/s42408-023-00237-9, 2024.

Scholten, R. C., Pendergrass, A. G., Abatzoglou, J. T., Xu, C., and Tchebakova, N. M.: Early snowmelt and polar jet dynamics co-influence recent extreme Siberian fire seasons, *Science*, **378**, 1005–1009, https://doi.org/10.1126/science.abn4419, 2022.

Scholten, R. C., Veraverbeke, S., Chen, Y., and Randerson, J. T.: Spatial variability in Arctic–boreal fire regimes influenced by environmental and human factors, Nat. Geosci., 17, 866–873, https://doi.org/10.1038/s41561-024-01505-2, 2024.

Scholze, M., Allen, J. I., Collins, W. J., Cornell, S. E., Huntingford, C., Joshi, M., Lowe, J. A., Smith, R. S., and Wild, O.: Earth system models: a tool to understand changes in the Earth system, in: Understanding the Earth System. Global Change Science for Applications, edited by: Cornell, S. E., Prentice, I. C., House, J. I., and Downy, C. J., Cambridge University Press, Cambridge, 129–159, 2013.

Scott, A. C. and Glasspool, I. J.: The diversification of Palaeozoic fire systems and fluctuations in atmospheric oxygen concentration, Proceedings of the National Academy of Sciences. USA, 103, 10861–10865, https://doi.org/10.1073/pnas.0604090103, 2006.

Seo, H. and Kim, Y.: Forcing the Global Fire Emissions Database burned-area dataset into the Community Land Model version 5.0: impacts on carbon and water fluxes at high latitudes, Geosci. Model Dev., 16, 4699–4713, https://doi.org/10.5194/gmd-16-4699-2023, 2023.

Teckentrup, L., Harrison, S. P., Hantson, S., Heil, A., Melton, J. R., Forrest, M., Li, F., Yue, C., Arneth, A., Hickler, T., Sitch, S., and Lasslop, G.: Response of simulated burned area to historical changes in environmental and anthropogenic factors: a comparison of seven fire models, Biogeosciences, 16, 3883–3910, https://doi.org/10.5194/bg-16-3883-2019, 2019.

Teixeira, J. C. M., Burton, C., Kelley, D. I., Folberth, G. A., O'Connor, F. M., Betts, R. A., and Voulgarakis, A.: Improving historical trends in the INFERNO fire model using the Human Development Index, EGUsphere [preprint], https://doi.org/10.5194/egusphere-2025-3066, 2025.

Tian, C., Yue, X., Zhu, J., Liao, H., Yang, Y., Lei, Y., Zhou, X., Zhou, H., Ma, Y., and Cao, Y.: Fire–climate interactions through the aerosol radiative effect in a global chemistry–climate–vegetation model, Atmos. Chem. Phys., 22, 12353–12366, https://doi.org/10.5194/acp-22-12353-2022, 2022.

Tian, H., Lu, C., Ciais, P., Michalak, A. M., Canadell, J. G., Saikawa, E., Huntzinger, D. N., Gurney, K. R., Sitch, S., Zhang, B., Yang, J., Bousquet, P., Bruhwiler, L., Chen, G., Dlugokencky, E., Friedlingstein, P., Melillo, J., Pan, S., Poulter, B., Prinn, R., Saunois, M., Schwalm, C. R., and Wofsy, S. C.: The terrestrial biosphere as a net source of greenhouse gases to the atmosphere, Nature, 531, 225–228, https://doi.org/10.1038/nature16946, 2016.

Tosca, M. G., Randerson, J. T., and Zender, C. S.: Global impact of smoke aerosols from landscape fires on climate and the Hadley circulation, Atmos. Chem. Phys., 13, 5227–5241, https://doi.org/10.5194/acp-13-5227-2013, 2013.

United Nations Environment Programme (UNEP): Spreading like Wildfire – The Rising Threat of Extraordinary Landscape Fires, A UNEP Rapid Response Assessment, Nairobi, 126 pp., https://www.unep.org/resources/report/spreading-wildfire-rising-threat-extraordinary-landscape-fires, 2022.

van der Werf, G. R., Randerson, J. T., Giglio, L., van Leeuwen, T. T., Chen, Y., Rogers, B. M., Mu, M., van Marle, M. J. E., Morton, D. C., Collatz, G. J., Yokelson, R. J., and Kasibhatla, P. S.: Global fire emissions estimates during 1997–2016, Earth Syst. Sci. Data, 9, 697–720, https://doi.org/10.5194/essd-9-697-2017, 2017.

van Marle, M. J. E., Kloster, S., Magi, B. I., Marlon, J. R., Daniau, A.-L., Field, R. D., Arneth, A., Forrest, M., Hantson, S., Kehrwald, N. M., Knorr, W., Lasslop, G., Li, F., Mangeon, S., Yue, C., Kaiser, J. W., and van der Werf, G. R.: Historic global biomass burning emissions for CMIP6 (BB4CMIP) based on merging satellite observations with proxies and fire models (1750–2015), Geosci. Model Dev., 10, 3329–3357, https://doi.org/10.5194/gmd-10-3329-2017, 2017.

van Marle, M. J. E. and van der Werf, G. R.: DRES-CMIP-BB4CMIP7-2-0, https://input4mips-cvs.readthedocs.io/en/latest/source-id-landing-pages/DRES-CMIP-BB4CMIP7-2-0/, (last access: 10 October 2025), 2025.

van Vuuren, D., O'Neill, B., Tebaldi, C., Chini, L., Friedlingstein, P., Hasegawa, T., Riahi, K., Sanderson, B., Govindasamy, B., Bauer, N., Eyring, V., Fall, C., Frieler, K., Gidden, M., Gohar, L., Jones, A., King, A., Knutti, R., Kriegler, E., Lawrence, P., Lennard, C., Lowe, J., Mathison, C., Mehmood, S., Prado, L., Zhang, Q., Rose, S., Ruane, A., Schleussner, C.-F., Seferian, R., Sillmann, J., Smith, C., Sörensson, A., Panickal, S., Tachiiri, K., Vaughan, N., Vishwanathan, S., Yokohata, T., and Ziehn, T.: The Scenario Model Intercomparison Project for CMIP7 (ScenarioMIP-CMIP7), EGUsphere [preprint], https://doi.org/10.5194/egusphere-2024-3765, 2025.

Verjans, V., Franzke, C. L. E., Lee, S., Kim, I., Tilmes, S., Lawrence, D. M., Vitt, F., and Li, F.: Quantifying CO2 forcing effects on lightning, wildfires, and climate interactions, Sci. Adv., 11,

eadt5088, https://doi.org/10.1126/sciadv.adt5088, 2025.

Ward, D. S., Kloster, S., Mahowald, N. M., Rogers, B. M., Randerson, J. T., and Hess, P. G.: The changing radiative forcing of fires: global model estimates for past, present and future, Atmos. Chem. Phys., 12, 10857–10886, https://doi.org/10.5194/acp-12-10857-2012, 2012.

Ward, D. S., Shevliakova, E., Malyshev, S., and Rabin, S.: Trends and variability of global fire emissions due to historical anthropogenic activities, Global Biogeochem. Cy., 32, 122–142, https://doi.org/10.1002/2017GB005787, 2018.

Whaley, C. H., Butler, T., Adame, J. A., Ambulkar, R., Arnold, S. R., Buchholz, R. R., Gaubert, B., Hamilton, D. S., Huang, M., Hung, H., Kaiser, J. W., Kaminski, J. W., Knote, C., Koren, G., Kouassi, J.-L., Lin, M., Liu, T., Ma, J., Manomaiphiboon, K., Bergas Masso, E., McCarty, J. L., Mertens, M., Parrington, M., Peiro, H., Saxena, P., Sonwani, S., Surapipith, V., Tan, D. Y. T., Tang, W., Tanpipat, V., Tsigaridis, K., Wiedinmyer, C., Wild, O., Xie, Y., and Zuidema, P.: HTAP3 Fires: towards a multi-model, multi-pollutant study of fire impacts, Geosci. Model Dev., 18, 3265–3309, https://doi.org/10.5194/gmd-18-3265-2025, 2025.

Wiedinmyer, C., Kimura, Y., McDonald-Buller, E. C., Emmons, L. K., Buchholz, R. R., Tang, W., Seto, K., Joseph, M. B., Barsanti, K. C., Carlton, A. G., and Yokelson, R.: The Fire Inventory from NCAR version 2.5: an updated global fire emissions model for climate and chemistry applications, Geosci. Model Dev., 16, 3873–3891, https://doi.org/10.5194/gmd-16-3873-2023, 2023.

Wu, C., Sitch, S., Huntingford, C., Mercado, L. M., Venevsky, S., Lasslop, G., Archibald, S., and Staver, A. C.: Reduced global fire activity due to human demography slows global warming by enhanced land carbon uptake, P. Natl. Acad. Sci. USA, 119, e2101186119, https://doi.org/10.1073/pnas.2101186119, 2022.

Xu, L., Zhu, Q., Riley, W. J., Chen, Y., Wang, H.-L., Ma, P.-L., and Randerson, J. T.: The Influence of Fire Aerosols on Surface Climate and Gross Primary Production in the Energy Exascale Earth System Model (E3SM), J. Clim., 34, 7219–7238, https://doi.org/10.1175/JCLI-D-21-0193.1, 2021.

Yu, Y. and Ginoux, P.: Enhanced dust emission following large wildfires due to vegetation disturbance, Nat. Geosci., 15, 878–884, https://doi.org/10.1038/s41561-022-01046-6, 2022.

Yu, Y., Mao, J., Wullschleger, S. D., Chen, A., Shi, X., Wang, Y., Hoffman, F. M., Zhang, Y., and Pierce, E.: Machine learning–based observation-constrained projections reveal elevated global socioeconomic risks from wildfire, Nat. Commun., 13, 1250, https://doi.org/10.1038/s41467-022-28853-0, 2022.

Yue, X. and Unger, N.: Fire air pollution reduces global terrestrial productivity, Nat. Commun., 9, 5413, https://doi.org/10.1038/s41467-018-07921-4, 2018.

Zhao, S. and Suzuki, K.: Differing Impacts of Black Carbon and Sulfate Aerosols on Global Precipitation and the ITCZ Location via Atmosphere and Ocean Energy Perturbations, J. Clim., 32, 5567–5582, https://doi.org/10.1175/JCLI-D-19-0001.1, 2019.

Zhao, Z., Lin, Z., Li, F., and Rogers, B. M.: Influence of Atmospheric Teleconnections on Interannual Variability of Arctic-Boreal Fires, Sci. Total Environ., 838, 156550, https://doi.org/10.1016/j.scitotenv.2022.156550, 2022.

Zheng, B., Ciais, P., Chevallier, F., Chuvieco, E., Chen, Y., and Yang, H.: Increasing forest fire

emissions despite the decline in global burned area, Sci. Adv., 7, eabh2646, https://doi.org/10.1126/sciadv.abh2646, 2021.

Zhong, Q., Schutgens, N., Veraverbeke, S., et al.: Increasing aerosol emissions from boreal biomass burning exacerbate Arctic warming, Nat. Clim. Change, 14, 1275–1281, https://doi.org/10.1038/s41558-024-02176-y, 2024.

Zou, Y., Wang, Y., Qian, Y., Tian, H., Yang, J., and Alvarado, E.: Using CESM-RESFire to understand climate–fire–ecosystem interactions and the implications for decadal climate variability, Atmos. Chem. Phys., 20, 995–1020, https://doi.org/10.5194/acp-20-995-2020, 2020.